N71-20503
NASA CR-117192

Interim Report

on

N.A.S.A. Grant No. N. G. R. 52-093-001

on

STUDIES ON ELECTROCHEMICAL FORMATION AND REDUCTION OF OXIDE FILMS ON NOBLE AND TRANSITION METALS

Project Director: Professor B. E. Conway

Senior Research Assistant: Dr. H. A. Kozlowska

Graduate Student: Mr. W. Sharp

University of Ottawa,
Department of Chemistry,
Ottawa 2, Canada.

Dated: 20th December, 1970

ABSTRACT

Surface oxidation of Pt electrodes has been studied in very pure solutions and various stages of the uptake of O by the surface have been resolved. The reversibility with respect to various stages in the formation and reduction of the surface oxide layer has been investigated in relation to the activity of the surface for organic oxidation reactions. The stages of surface oxidation are related to the geometries of various sub-lattices of O on the Pt surface rather than to specific stoichiometries of platinum-oxygen surface compounds. Work on single crystal Pt surfaces is now being undertaken.

Optical studies by means of ellipsometry show that in pure solutions and with sensitive instrumentation there is no distinguishability, with respect to potential dependence, between the change of optical properties and the change of the surface coverage determined by surface coulometry. There is, in fact, a close correlation down to the lowest coverages that can be detected at ca. 0.8 V, contrary to what has been reported in earlier literature. The present results agree in this respect with recent conclusions from the work using the modulated reflectance technique.

The experimental procedure for investigating Pt surface oxidation up to elevated temperatures has now been developed further and in particular, a satisfactory special type of autogenous H_2 electrode for use in a closed bomb has been fabricated and tested.

INTRODUCTION

The general aims of the work (indicated in earlier reports) have been to examine: (a) the stages of formation and reduction of oxides on noble metal surfaces in relation to the intermediates involved in oxygen reduction (and evolution) in aqueous solution; (b) how the oxidation and reduction of noble metal surface oxides depends on temperature, including high temperatures into the range of superheated water at elevated pressures; (c) the reversibility of the various stages of surface oxidation with respect to anodic and cathodic directions of potential change at the electrode.

The various stages of oxidation of noble metal surfaces and the question of the kinetics of the reduction of the corresponding surface oxide(s) is not only of interest in relation to the kinetics of molecular oxygen reduction but is also closely related to the various processes that can arise in the electro-oxidation of small organic molecules of interest in fuel-cell technology.

Experimentally, the potential sweep or potentiodynamic method is capable of giving the best resolution of the various stages of surface oxidation of metals because it is, in effect, a differential method. Provided the range of potentials covered in a sweep is between the thermodynamic reversible potentials for H_2 and O_2 evolution, the analysis of the resulting current(i)-potential (V) profiles does not involve any ambiguities in principle; the integrals $\int i\,dt$ or $\int \frac{i}{s}.dv$ where s is the (linear) sweep rate dV/dt, taken between any two potentials or corresponding times, give accurately the charge passed only for formation

or removal of surface oxide species or, at more negative potentials, adsorbed H species. The theory of the method for surface species was treated first by Conway[1], by Gileadi and Srinivasan[2] and by Stonehart, Kozlowska and Conway[3] for the case of Pt.

EXPERIMENTAL APPROACHES

The main experimental approaches have been as follows:

(a) Development of high purity conditions so that the various stages of surface oxidation, e.g. of Pt can be resolved as best as possible. From the present work it has become evident that results reported in various earlier publications in the literature were obtained in insufficiently pure solutions so that resolution of the oxidation behavior of Pt was inadequate and the corresponding stages of surface oxidation were incompletely revealed. The careful work that was carried out by Schuldiner[4] is an important exception to this statement but he concentrated on the use of the galvanostatic charging method which, without coupled differentiation[5], does not give significant resolution of the oxide formation process on Pt. In fact, he concluded that the slope of the charging curve was constant at Pt in the oxide formation region. This is incorrect.

(b) Development of a technique for high temperature measurements suitable for electrode-kinetic studies in a high pressure vessel up to ca. 250 - 300°C. This has necessitated (i) the design and construction of a compact three-compartment cell suitable for inclusion in

a 5" diameter pressure bomb provided with electrode and thermocouple leads, and (ii) the development of a reversible electrode system capable of being controlled internally in the cell without admission of gases from the exterior.

(c) Use of various types of controlled potential programs with particular reference to employment of linear potential sweeps applied after controlled periods of holding at various fixed potentials and at various sweep rates. The latter approach was important since time effects in the oxidation of noble metal surfaces are of great importance (cf. [3]).

EXPERIMENTAL DETAILS

(a) Electrodes: Spectroscopically pure Pt wires were sealed in glass bulbs in H_2 after annealing for 30 min. at 800°C in this gas. The wires had previously been degreased in acetone under reflux for 24 h. Platinized platinum and Pt sheet electrodes were also used but the results were identical on all three types of electrodes except that the wire electrodes were more sensitive to the influence of impurities, if they were present.

(b) Solutions: 1 N aq. H_2SO_4 solutions were made up from B.D.H. analytical grade, pure sulfuric acid and triply distilled water, the last distillation being made from a special glass apparatus in the presence of purified N_2. The use of the B.D.H. acid is important as other sources of acid give impurity currents at Pt. The

solutions were finally purified by cathodic and anodic preelectrolysis for 15 h at ca. 10^{-3} A.cm^{-2}. The solution was considered "pure" if holding the electrode at the cathodic end of the potentiodynamic sweep (+0.1 V E_H) for 1 - 2 minutes did not produce any change in the i-V profile except a slight increase of one of the H peaks (see below) and a slight increase of the first Pt oxidation region.

In between the runs, the electrode and the cell were cleaned with hot concentrated sulfuric acid, rinsed repetitively with double distilled water and kept in double distilled water.

Work in alkaline solutions has been described in previous reports arising from this project[6].

(c) Gases: N_2 and H_2 gases used for bubbling in the cell were purified as described in previously published papers[7].

(d) Cell and vessel for high temperature work: The design and construction of the cell and high temperature bomb vessel have been described in previous reports[6]. Apart from a special compact arrangement of the cell, the design follows the conventional layout[7] except for the reference electrode system described below.

(e) Design of a modified Giner type reference electrode: In a previous report, we have described preliminary experiences with various types of reference electrode in relation to their performance at elevated temperatures. An α/β Pd/H reference electrode was tested but worked satisfactorily only up to ca. 90 ^{o}C. Above this temperature, and in some experiments below this limit, its reliability was questionable.

In our previous reported studies of the oxidation and reduction of noble metal surfaces , potentiodynamic circuitry was used to vary the potential difference between the working electrode and a hydrogen reference electrode according to a preset triangular waveform. However, the autoclave in which the present high temperature oxidation studies are being made cannot have facilities for the introduction and removal of gaseous hydrogen required for the hydrogen electrode. It was therefore hoped that a reference potential could be obtained from an autogenous Pt electrode of the type described by Giner[8], rather than from another reference system, e.g. Hg/Hg_2SO_4, which could contaminate the solution with other ions.

A Giner autogenous platinized H_2 electrode[8] was therefore tested but control of the electrode over a wide range of temperatures was found to be difficult owing to uncertain polarization effects and its susceptibility to the influence of stirring was appreciable. In some cases, variations of as much as ± 20 mV were encountered depending on the driving current employed and any agitation or convection in solution.

Giner passed a current of 1 $mA.cm^{-2}$ between two platinized Pt foil electrodes, with the anode fixed 10 - 20 mm above the cathode in a compartment separated from the rest of the cell by a glass frit. A similar type of cell was constructed for the present work, with the frit replaced by a closed stopcock as in the cell made for the autoclave and a Luggin capillary added so that the potential of the Giner cathode could be measured directly against a conventional H_2 electrode. Some of the data obtained are compared with Giner's

results in Figs. 1 and 2. The main reason for the discrepancy between the results is thought to be the easier diffusion of oxygen to the cathode in the present case where Pt gauze electrodes were used instead of foil, although the IR drop in Giner's cell may have differed from that in the present cell. The times required for the system to reach an "equilibrium" or steady potential were, however, similar to those quoted by Giner. The potentials shown are steady values reached minutes after presaturating the solution with hydrogen. However, they gradually begin to drift anodic unless the cell current is maintained at above about 0.3 mA cm^{-2}. With a steady current of 0.3 mA. cm^{-2}, the reference potential was stable within ± 1 mV over a period of 3 days. Cell currents of above about 0.3 mA. cm^{-2} gave rise to irregular fluctuations in cathodic potential between apparently fixed limits; the mean values are shown. Fluctuations are due to formation of bubbles.

The stationary potentials at different cell currents were not simple functions of the cell temperature probably because more than one parameter was varying simultaneously, e.g diffusion and ionization of oxygen and hydrogen, bubble size, convection etc.

Finally, it is noteworthy that, at all currents studied, the bubbling of hydrogen through the reference compartment was found to reduce the measured cathodic overpotential. This effect has been studied in detail by Ludwig and Yaeger [Office of Naval Research, Contract No. N00014-67-C-0389, Project No. NR 359-277, Technical Report No. 21 (1968)], who consider that bubbles near the electrode surface reduce the hydrogen supersaturation thereby allowing dissolved gas to enter the bubble and thereby reduce the overpotential.

This work emphasized that the behavior of the hydrogen-evolving cathode in the Giner reference system is not simply related to that of the ordinary H_2 electrode and studies at intermediate temperatures showed that its potential does not exhibit a simple relationship to tem perature.

(f) Performance of a new type of reference electrode system: A new type of reference electrode was therefore designed in which H_2 could be generated electrolytically in situ at a cathode consisting of a small platinized platinum gauze cylinder. The H_2 evolved then established the reversible potential at a platinized wire, mounted separately within the cylinder, which was on open circuit with respect to the working electrode and the H_2 generating system. Polarization effects were therefore absent and no stirring problems were involved. A small auxiliary counter-electrode, higher up inside the reference electrode compartment, enabled current to be passed at the H_2 generating electrode. Two Luggin capillaries were provided to shield off currents passing and minimize "IR" resistance polarization, one to the H_2 reference electrode within the gauze cylinder and the other to the usual working electrode. This arrangement works excellently up to elevated temperatures and the only factor which requires control is the cathodic current at the H_2 generating cylinder; larger currents up to 1 mA are required at the higher temperatures than at the lower, where 0.1 mA is sufficient to maintain excellently stable reference potentials.

The environment of the wire was rapidly saturated by the hydrogen being produced all around it and the cylindrical cathode apparently acts as a getter for the reduction of any oxygen diffusing downwards from the anode. Cell currents of above about 0.1 mA.cm^{-2} gave steady wire potentials (e.g. with 1 mA.cm^{-2} the potential was -1 mV ± 1 mV over 20 h). However, currents higher than 1 mA.cm^{-2} caused the type of potential fluctuation described above, as large bubbles of hydrogen were seen to form, grow and escape from the cylinder. These fluctuations were not avoided by tilting the cylinder from the horizontal, nor by making it shorter and wider, which resulted in more cathodic potentials being observed like those found with the Giner electrode.

The potential fluctuations were considerably reduced by packing the space between the reference wire and the cathode cylinder with Pyrex wool. This prevented the formation of sizeable hydrogen bubbles on the cathode, yet did not hinder the saturation of the solution it contained. The potential fluctuations observed, which had a cycle time of 10 - 500 s were then only ± 0.7 mV with 4 - 8 mA.cm^{-2}, ± 0.3 mV with 1 - 3 mA.cm^{-2} and ± 0.6 mV with 0.2 - 0.5 mA.cm^{-2}. Stability of the potential was maintained over long periods, e.g. with a current of 1 mA.cm^{-2} it was -0.9 mV ± 0.3 mV over a period of 60 h.

When the cell temperature was raised, the reference potential became rather less reproducible (Fig. 3) although the individual fluctuations and drift were of the same magnitude. With currents of less than 0.5 $mA.cm^{-2}$, however, the potential was unstable and drifted rapidly anodic, presumably as a result of the increased diffusion of hydrogen away from the cylinder and of oxygen into it at the higher temperatures. Currents greater than this value produce, however, a satisfactorily stable potential at 95°C and higher.

It has been established that this 3 electrode reference system may be used to control potentiodynamic sweeps on a noble metal electrode, and the first satisfactory results of the effect of heating Pt in 1 M H_2SO_4 on its oxidation-reduction behavior are shown in Fig. 4.

RESULTS AND DISCUSSION

Form of potentiodynamic current-potential profiles

In the case of acid solutions, it is important to establish if any structure in the oxidation current-potential for the surface oxide formation region is dependent upon the type of anion in the solution. Measurements were therefore made in 1 N sulfuric acid and 1 N perchloric acid and are compared in Figures 5a and 5b. It is evident that the same peaks can arise but the resolution is not so good as in sulfuric acid solution, probably because perchloric acid is more difficult to purify than is sulfuric; for example, the hydrogen peaks at more cathodic potentials may be compared and evidently are less well resolved. Only the first peak in the surface oxide formation region is seen to be somewhat better resolved in the perchloric acid solution.

The principal behavior to be noted in Figures 5a and 5b, which is also illustrated in Figure 6, is the development of two main peaks at the beginning of the surface oxide formation region above a potential of 0.94 V together with a preliminary peak at 0.89 V.

These peaks are shown on a larger scale in Figure 6 where they are designated* in order of appearance with increasing potential, as "OA0", OA1" and OA2", the latter being followed by a broad region continuing into the range of potentials where oxygen molecule evolution

---

* The designations refer to "oxide, anodic" peaks 0, 1 or 2; and the H peaks as "hydrogen cathodic", 1 and 2 or "hydrogen anodic", etc.

eventually becomes significant. At the cathodic end of the sweep, proceeding in a cathodic direction, the normal two hydrogen peaks indicated as "HC 1" and "HC 2" are seen while on the anodic direction of the cycle a third hydrogen peak is reproducibly observed and is indicated as "HA 3". The small peak HA3 only appears after the electrode has been either held at the reversible hydrogen potential or if the potential range includes the region + 0.1 V to 0.0 V. The familiar single peak in the cathodic reduction profile indicated as "OC", corresponds to the reduction of the surface oxide formed in the anodic direction of the sweep. The hysteresis, referred to in our previous publications[3,9], is to be noted. This matter is of some importance in connection with the reversibility of various stages of the oxide formation and reduction, referred to below, when limited ranges of anodic potential are covered, that is lower than the limits shown in Figure 6.

Reference to Figures 5a and 5b and to Figure 6 indicates clearly the presence of three surface oxide formation regions which are formally similar to the regions observed at more cathodic potentials with respect to hydrogen adsorption. They may correspond to different types of oxygen species on the surface or to adsorption on different types of sites available. However, it might be expected that the current potential curve should be more or less symmetrical in the cathodic and anodic directions in the case of intrinsic heterogeneity, with the oxygen being adsorbed on various types of sites with three reduction peaks also being observed in the cathodic sweep. This is never observed at slow sweep rates and two peaks are only observed at high sweep rates if the potential has been taken above about 1.5 V.

It therefore appears that the resolution into three distinguishable oxidation stages which is possible in sufficiently purified solutions is, in effect, connected with successive stages of the oxidation of the surface and the related interactions between the O or OH species laid down with increasing potential. The peak potentials are summarized below.

Table I

Peak designation	Peak potential E_H, V.
O_{A0}	0.89 V
O_{A1}	0.94 V
O_{A2}	1.05
Broad region	1.2 V into O_2 evolution region

A further indication of distinguishable species upon the surface at potentials higher than about 0.8 V is given by the fact that various organic substances show characteristic Faradaic peak currents corresponding to the various regions of surface oxide formation shown in Figures 5 and 6. In Figure 7 is shown the typical behavior observed for formic acid oxidation at platinum in acid solution where three main Faradaic oxidation peaks appear; the first one indicated as "FA 1" appears in the double-layer region and is not connected with the presence of surface oxide formation. The first peak in the oxide

formation region "FA 3"* appears to arise because of reaction with the oxide species on platinum corresponding to the regions OA0 and OA1. Inhibition of the current beyond a potential of about 1.05 V seems to be connected with the development of the oxide in the OA2 region. The theory of these effects has been given previously[10]. This inhibition persists up to about 1.2 V whereupon a third region of Faradaic oxidation indicated by "FA 4" in Figure 7 arises. It seems that this oxidation is one connected with the broad region of surface oxide formation beyond about 1.2 V. It is interesting to note that the two main regions of oxidation typified by FA3 and FA4 for formic acid are also observed with other related substances such as methanol and formaldehyde, for example as discussed by Vielstich[11]. The peak potentials and the potential range of the current minimum in Figure 7 are summarized in Table 2. Another indication of the distinguishability of the first two oxide peaks on platinum from the region at higher potentials is given in Figure 8 which shows the behavior of platinum surface oxidation in the presence of acetonitrile. The acetonitrile not only blocks the hydrogen region, as may be expected, but exhibits an oxidation behavior in the double-layer region which, as shown elsewhere, corresponds to a chemisorbed species on the surface. In addition to these effects, and of interest in the present context, there is an important blocking of the formation of the surface oxide on platinum in the regions OA0 and OA1; at higher potentials, in the OA2 region, there is, however, some reaction between the acetonitrile and the oxide. The diminution of the oxide coverage can readily be seen on the reduction profiles in the OC region in the cathodic sweep. The effects are quite appreciable.

---

* Under other conditions, a peak we designate as FA2 appears but it is not discussed further here.

Table II

Faradaic peak designation	FA1	FA3	Current minimum	FA4	FK_2	FK_1
Peak potential E_H, V	0.55	0.94	1.05-1.16	1.53	0.63	0.46
Corresponding oxide peak	-	O_{A0}, O_{A1}	O_{A2}	broad region		

Reversibility at various stages of surface oxidation

In order to study the reversibility of formation and reduction of the surface oxides and hence to gain some further insight into their reactivity in oxygen reduction and in fuel-cell oxidation processes, potential sweeps were made to various anodic termination potentials as shown in Figure 9. Considering the behavior towards progressively increasing anodic potentials, it is to be noted that in the initial stages of surface oxidation towards the region OA 0 (Figure 9), an anodic sweep terminated at about 0.85 V and reversed gives an immediate fall of the current and a corresponding cathodic peak at the same potential in the reverse direction of sweep; this behavior is characteristic of almost reversible oxidation and reduction. Progression to a somewhat higher anodic potential, but still in the OA0 region, results in the second curve which shows again an immediate drop of current upon reversal of the sweep with a peak formed in the cathodic direction of the sweep; this peak appears at more anodic potentials than the first one corresponding to a greater amount of the species formed on the surface; this is as

expected. Further progression of the anodic termination potential in the region of OA1 results, however, in a slightly different behavior in which irreversibility is beginning to be exhibited; for example, the peak potential now returns to a somewhat more cathodic value and there is a different shape of the cathodic sweep curve. By the time the fourth curve is reached at higher anodic potentials again, a greater irreversibility is exhibited and a further progression of the cathodic peak to more negative potentials is observed. It is seen that irreversibility is beginning to set in between the formation and reduction of the species formed up to a potential of 0.95 V. For the remaining curves obtained from successively higher polarizations to progressively more positive termination potentials, it is seen that the irreversibility increases as indicated by the hysteresis between the anodic-going and cathodic-going current profiles.

An interesting aspect of the behavior for polarizations at the higher anodic potentials is that upon reversal of the sweep the current does not immediately become a cathodic one as it does in the hydrogen or double-layer regions, but a region of remaining anodic current persists in the cathodic sweep until the sweep has passed back to significantly more negative potentials. It therefore appears that anodic oxidation of the surface continues during the initial stages of cathodic sweeps for termination potentials higher than about 1.0 V. In fact, it seems that the whole of the cathodic-going current-potential profiles, almost up to the cathodic peak OC, can be represented as a Faradaic reaction process corresponding simply to the diminution of amount of surface oxide species with increasing cathodic potential as for example treated in reference 3.

Figure 9 also shows the integrated oxide charge expressed as the ratio Q_O/Q_H as a function of anodic potential. It is of interest that this ratio attains a value of unity already at a potential of 1.12 V. The significance of this important observation will be discussed further below. It is also seen from Figure 9 that beyond the critical ratio $Q_O/Q_H = 1$, the slope of the integrated charge-potential line becomes somewhat less. The relation between the potentiodynamic current potential profile in Figure 9 and the integrated charge profile illustrates a general difficulty which arises in interpretation of integral charge-potential relations. It is readily seen that the Q_O/Q_H line shows very little structure in relation to that indicated differentially by the current-potential profile itself. This has an important bearing on the choice of experimental methods for study of surface oxide species as mentioned in the Introduction; for example, it is obviously undesirable to use a direct charging curve method such as has been employed by Schuldiner even if the solutions are sufficiently pure that difficulties concerned with impurity oxidation or blocking behavior are avoided. Only by the differential galvanostatic method[5] can one hope to see any structure in the charging curve, or preferably by use of the potentiodynamic method one can see directly the differential charging behavior. Similar considerations apply to the potential step charging method recently investigated by Urbach et al[13].

We have referred[12] above to another aspect of the oxidation kinetics as illustrated by the behavior of the current potential profiles in Figure 9, particularly those corresponding to high anodic termination potentials. It was seen that upon reversal of the sweep to a cathodic direction, there is a remaining anodic current passing.

This must correspond to a slow continuing oxidation of the surface until a potential sufficiently far removed in the cathodic direction from the previous anodic termination potential is attained that reduction of the oxide species formed at the highest anodic potentials can commence.

In Figure 10 is shown the effect of the anodic termination potential E_a on the oxide reduction behavior in two ways: (a) the dependence of the peak potential for cathodic reduction on E_a ; and (b) the relation of the cathodic peak potential to the oxide coverage expressed in terms of the ratio Q_O/Q_H. It is seen that initially, in the range of potentials where the oxide formation and reduction is almost reversible, that the cathodic peak potential becomes more positive with increasing anodic termination potential or amount of surface oxide formed; however, for $E_a \gtrsim 0.9$ V, the cathodic peak potential begins to decrease progressively until a potential of about 1.04 V is reached in the anodic termination potential. After this region, as seen in Figure 10, there is a range of surface coverage over which the cathodic peak potential remains almost constant with increasing amount of oxide coverage, up to an anodic termination potential of about 1.17 V. Reductions of oxide formed to higher potentials then show cathodic peak potentials which become more negative with increasing oxide coverage in the manner previously reported by Stonehart, Kozlowska and Conway[3].

It is interesting to speculate that the region where the cathodic peak potential remains independent of the amount of oxide coverage may be related to the fact that two surface oxide phases are formed on the surface and there is equilibrium between them, thus giving a potential independent of the amounts of either until one or the other is completely removed from the surface.* Two possible explanations

* Other experiments in this laboratory have shown that in the potential range $1.08 < E < 1.2$ V, dermasorbed O is formed which can be detected by its influence on formic acid oxidation in the double-layer region. The region of constant peak potential may hence correspond to entry of some of the electrodeposited O into the Pt lattice.

may be given for the increasingly cathodic peak potential which arises with increasing amount of oxide coverage beyond that corresponding to a potential of ca. 1.18 V. First of all, this may simply represent progressively increasing hysteresis[3, 9] corresponding to lower potentials for reduction being required for that part of the oxide which is laid down at higher anodic potentials. This sort of effect could arise, for example, on account of rearrangement of the surface oxide species. A second possibility, connected simply with the amount of substance formed, may be suggested in relation to the cathodic current-potential curves for reduction of oxide formed at the most anodic potentials shown in Figure 9. Here it appears that there is a more or less common cathodic reduction current-potential curve and this is simply able to persist to more cathodic potentials when there is a greater amount of reducible oxide present. This then gives a peak which is observed at more cathodic potentials the greater the amount of substance formed in the anodic direction. For example, the cathodic current-potential curve will persist until something like half coverage of the oxide remains and then of course the currents must decrease again even though the cathodic driving potential is progressively increasing during the cathodic sweep.

In considering the results of Figure 10 in relation to those of Figure 9, it should be noted that the relation between the cathodic peak potential and the anodic termination potential plotted on the upper axis of abscissae is shown on a non-linear scale in order to represent the appearance of the various peaks at the corresponding coverages shown in terms of Q_O/Q_H on the lower axis of abscissae.

Sweep rate effects in relation to reversibility

The reversibility of the formation and reduction of the surface oxide species on platinum has been indicated in Figures 9 and 10 in terms of the cathodic peak potential in relation to the various anodic peak potentials for the formation of successive states of the surface. Another aspect of the reversibility can be indicated by studying the dependence of the cathodic peak potential upon cathodic sweep rate[9]. For an activation controlled process, it may be anticipated that the peak current, which must increase for a surface reduction process with the sweep rate, will cause an increasing polarization in the cathodic direction with increasing cathodic current passed if the process is irreversible. One may thus anticipate that there is a cathodic polarization shift dependent upon the log of the sweep rate. This was shown in earlier studies of cathodic reduction of platinum surface oxides by Gilroy and Conway[9]. In the present work, we have investigated this matter further by examining the dependence of cathodic peak potential upon logarithm of the sweep rate for various amounts of oxide formed, that is corresponding to various anodic termination potentials. The results are shown in Figures 11 and 12. It is seen that the initial species laid down in the anodic direction is reduced, in terms of this criterion, in a more or less reversible way; for example, there is no dependence of cathodic peak potential on sweep rate. However beyond about 0.93 V in the anodic formation of the surface oxide species, cathodic reduction results in a sweep-dependent peak potential E_p having a slope $d E_p / d \log s$ which increases with increasing amount of surface oxide, as formed, for example, up to progressively higher anodic potentials. In all cases, there seems to be a quite satisfactory linear logarithmic relationship, that is a Tafel type relation, between the cathodic peak potential and log of the sweep rate. In Figure 12, the results of Figure 11 are shown as Tafel slopes $d E_p / \log s$ as a function of the anodic termination potential.

It is seen that there is a progressive increase of the Tafel slope with increasing anodic termination potential and it is evident, within the uncertainties of the measurements at low coverages, that the formation and reduction of the surface oxide is effectively reversible up to about 0.93 V in terms of the observed kinetic behavior. This is also seen in the initial curves of Figure 10.

A more accurate indication of the dependence of Tafel slope for the reduction process is given by the results of Figure 13. In Figure 12, the relation between cathodic peak potential and anodic termination potential had been obtained in multisweep experiments in which both the anodic and cathodic sweep rates had been changed uniformly. Owing to time effects in the oxide formation, the amounts of oxide formed at various anodic termination potentials depend upon the anodic sweep rate. The data in Figure 13 were obtained by using a constant anodic sweep rate of 1 V per sec. but with a varying cathodic sweep rate. The data shown indicate that the Tafel slope expressed by the dependence of the cathodic peak potentials on log of sweep rate now increases progressively up to a value of 25 mV with increasing anodic termination potential to a limit of E_a = ca. 1.18 V. At potentials more anodic than this termination potential, namely up to about 1.6 V, the Tafel slope remains constant at the value of 25 mV, despite the fact that the amount of oxide formed up to these progressively increasing potentials itself is continuously increasing.

Slowness in the oxidation and reduction processes: the result of holding the potential prior to cathodic or anodic sweeps

A number of experiments were conducted in which cycling between various ranges of potential was conducted. Figure 14a shows the behavior for repetitive cycling between a succession of cathodic potentials up to an anodic termination potential of about 1.27 V. From curve c to curve g there is little effect of cycling time. However, if the cycling is carried on within the region of formation and reduction of the oxide (curves h and i) there is a progressive decrease of the anodic formation charge Q_O and the cathodic reduction charge with increasing time of cycling. In the case of curve i with cycling from 0.9 V to 1.27 V, hardly any anodic or cathodic charge is indicated and the curve approximates simply to that for double-layer charging. In fact, this approach can give an indication of the double-layer capacity for the oxide covered surface. It is evident that both the slowness of the anodic oxide formation process and the corresponding reduction process leads to a progressively diminishing available (from an electrochemical point of view) amount of oxide on the surface. Thus, the oxide remains on the surface within this region and indeed its reduction is indicated only if a sweep back into more cathodic regions of the potential is made from the highest anodic termination potential after the cycling procedure. It simply becomes inactive within the potential range cycled in the cases of curves h and i. Slowness of the cathodic reduction of the oxide is also indicated by the fact that even at the cathodic end of the cathodic sweep, when the direction of sweep is reversed, a cathodic current still continues to pass over a small range of potentials in the anodic sweep. In Figure 14b,

repetitive cycle experiments are shown from three potentials in the more cathodic region to 1.27 V and it is evident that in the oxide formation and reduction regions the charge remains constant during successive cycles. However, the commencement of slowness of reduction of the surface oxide remaining at 0.55 V is already indicated in curve c. Extension of the range of cathodic reduction to + 0.01 V causes no further influence on the oxidation-reduction behavior of the oxide.

The effects of holding the potential anodically for various times and then applying single cathodic sweeps to examine the reduction behavior of the oxide previously formed, are shown for three anodic potentials in Figures 15a, b and c. In reduction curves obtained from an anodic termination potential of 0.9 V, it is seen that there is an initial, fairly reversible peak but the peak potential gradually becomes progressively more cathodic with increasing time of holding up to 30 minutes. In Figure 15b, with anodic holding at 0.95 V, there is again a fairly reversible peak but the peak potential progressively moves cathodically with time and, furthermore, the total amount of charge (as also probably in Figure 16a), increases appreciably with time of anodic holding, again up to 30 minutes. In the case of anodic holding at 1.0 V, Figure 15c shows the behavior where there is already some irreversibility between the anodic formation process and the cathodic reduction and again there is a progressive movement of the cathodic peak potential with time of anodic holding and there is also appreciable growth of the amount of oxide as measured by the charge under the reduction curve. It is of interest to note from Figure 15c that the shift

of cathodic reduction peak potential with quantity of surface oxide formed, and hence with time, is substantially less than in the cases of Figure 15a and 15b where the amounts of oxide formed are smaller. This, however, corresponds with the behavior shown in Figure 10 where the cathodic peak potential for various stages in the surface oxide formation was related to the integral charge on the surface expressed as Q_O/Q_H. In fact, the behavior in Figure 15c is approaching that corresponding to the plateau in Figure 10 where the cathodic peak potential is about 0.8 V. It is evident, for example in Figures 15a and 15b, that although only the initial stages of surface oxidation of the platinum are involved, there is nevertheless an appreciable time effect with regard to continuing growth and/or rearrangement of the surface species forming the oxide film. It may be suggested, as has been noted in our earlier publications, that the possibility exists that nucleation processes are involved in these time effects; thus, islands of more consolidated surface oxide may eventually be formed which require more cathodic potentials for their reduction, determined by the greater amount of substance eventually produced in these islands with increasing time, corresponding to the anodic holding period. It is evident upon comparing Figures 15c with 15b and 15a that the shift of cathodic peak potential is not solely connected with the amount of species concerned. For example, as we have remarked above, it is evident that the initial species laid down, indicated in Figures 15a and 15b, exhibit a greater progressive change of the peak potential for their cathodic reduction than does the larger amount of substance produced at the higher potential (1.0 V) (Figure 15c). This again lends

support to the view taken in this report, and mentioned earlier, that there are distinguishable species upon the surface each exhibiting its own characteristic behavior.

The results of the holding experiments at various anodic termination potentials on the behavior of the cathodic reduction peak are illustrated in another way in Figure 16 where the peak potential has been plotted against the surface oxide coverage expressed in terms of the ratio Q_O/Q_H over various regions. For low anodic termination potentials of 0.9 and 1.0 V, the cathodic peak potential shows a progressive diminution with increasing surface oxidation corresponding to increasing times of anodic holding. For a potential of 1.1 V in the anodic holding, the cathode peak potential exhibits, however, a fairly constant region as the degree of surface oxidation increases with time. This constancy is also indicated by the lower coverage results for polarizations up to 1.2 V. However, the data for longer times and correspondingly larger coverages for this potential of 1.2 V, and all the data for holding experiments at 1.4 V, show a further progressive change of E_p to more cathodic potentials with time at the higher coverages. The latter effect is similar to that observed in the previously published work of Stonehart, Kozlowska and Conway[3] and as also indicated in Figure 10 for the cyclic sweep experiments without anodic holding. Again, the plateau in the intermediate region is suggestive of the joint effect of two types of surface oxide species which show characteristically different dependencies of the cathodic peak reduction potentials with respect to the amounts of the species present on the surface; that is, there is either a mixed potential involved or a situation where two surface phases coexist over a certain range of coverages and corresponding potentials. This may correspond to "OHPt" and "O2Pt" as discussed below.

Relation between behavior in acid and alkaline solution

In previous reports we have indicated the behavior in alkaline solutions and referred to the fact that there are again three distinguishable oxide formation regions on platinized platinum, together with a new region which appears in the anodic sweep in the double-layer region, that is about 0.65 V. The significance of this peak is still under investigation using specially purified solutions and a Teflon cell. The behavior has, however, been reproducible and leads to the question whether there is not, in fact, a new initial state of surface oxidation on the platinum electrode in alkaline solutions which does not appear in acid solutions over corresponding ranges of potential. The general behavior in Figure 17, expressed as the integral charge Q_O/Q_H, shows simply that a given potential the surface takes a greater degree of oxidation in alkaline than in acid solutions; for example, significant commencement of surface oxidation is already detectable at 0.6 V in alkaline solutions whereas it is only detectable in acid solutions at about 0.75 V. It is of interest that in the present work the commencement of the surface oxidation as determined by charging measurements based on the potential sweep method compares closely with indications of the appearance of surface oxide measured by means of ellipsometry. There is evidently no contradiction between the behavior observed coulombically and optically as has been claimed in earlier work by Bockris and Genshaw[14] and in polemics with Greef[15] and others.

Summary of evidence for distinct stages of the oxidation of the Pt surface

At this stage of the report it will be useful to summarize the evidence for distinct species, electrochemisorbed at oxidized Pt surfaces in contrast simply to heterogeneity of the surface. The potentiodynamic i - V curves are differential charging curves insofar as the current passing at any potential in a sweep is $i_V = \frac{dq_v}{dt} = s\, dq_v/dV$, i.e. the current is proportional to the differential pseudo-capacitance where s is the sweep rate. Inflections in a charging curve appear as maxima or minima in the potentiodynamic curve which therefore represent inflections in the electrochemical isotherm for potential dependence of coverage by the ad-species. The question arises whether these inflections are due to adsorption on different types of metal sites (intrinsic heterogeneity), whether they correspond to progressively different stages of oxidation of otherwise similar atoms in the metal surface or whether the effects arise because various sub-lattices of O-species are formed in two dimensions on the electrode surface as indicated by LEED studies in the case of O adsorbed from the gas phase, e.g. on to Ni. Changing interactions will also be connected with the types of two-dimensional surface lattices set up as the coverage increases, e.g. due to dipole-dipole interactions and the "induced heterogeneity" effects described by Bourdart which arise because changes of surface-potential modify the electronic work function of the metal and hence cause the energy of chemisorption of O species to be dependent on coverage.

A real difference of type of species (in distinction to intrinsic heterogeneity* due to crystal face exposures as the potential of Pt is made more anodic seems to be indicated by the results presented above, e.g. with respect to (a) reversibility; (b) shifts of cathodic reduction peak potentials; (c) the distinct potential ranges in which simple organic substances are oxidized or in which this oxidation is inhibited.

The problem of accommodation of charge passed in various stages of Pt surface oxidation

If the above conclusions are accepted, there remains the problem of describing various possible states of oxidation of the Pt surface in terms of appropriate chemical oxygen species in relation to the charge passed in the anodic sweep up to various potentials. The first principal peak OA1, already appears at a potential where $Q_O/Q_H < 0.5$ and it is tempting to ascribe it to oxidation of the surface by chemisorbed OH species. Even at the peak of the OA2 region, less than 1 e per Pt atom has been passed. This situation is very difficult to account for in terms of two separate and independent stages of surface oxidation of Pt such as

$$Pt + H_2O \rightarrow \text{"PtOH"} + H^+ + e \qquad \text{I}$$

followed by

$$PtOH \rightarrow \text{"PtO"} + H^+ + e \qquad \text{II}$$

* Further experiments are in progress concerning intrinsic heterogeneity effects, using single crystal Pt electrodes kindly loaned to us by Dr. F. Will of the General Electric Company.

where the quotation marks stress that the species indicated do not necessarily correspond to any real bulk substances of such stoichiometry. In order to account for two main peaks close together with the maximum in the first peak corresponding to $Q_O/Q_H \leqslant 0.35$ we suggest that the initial stage of surface oxidation is indeed I but that coverage by 'OH' species does not proceed to completion owing to occurrence of another reaction which causes further oxidation of the surface yet inhibits continuing oxidation by the 'OH' species produced in I. Such a reaction on the incompletely covered surface could be

$$PtOH + Pt \rightarrow \begin{matrix} Pt \\ \diagdown \\ O \\ \diagup \\ Pt \end{matrix} + e + H^+ \qquad \text{III}$$

which corresponds to a continuing oxidation yet will provide a kinetic peak, as well as inhibiting I, since the kinetics of III may be written

$$i_3 = F\, k_3\, \Theta_{OH}(1-\Theta_{OH}) \exp \beta V F/RT \qquad (1)$$

When the surface is "completely" covered in terms of an O>2Pt arrangement, 1 e per Pt will have been passed, i.e. $Q_O/Q_H = 1$. This also corresponds to kinetic blocking of organic oxidation reactions in this range of potentials (1.0 - 1.2 V). Further oxidation of the surface may then proceed in the broad oxidation region ($\sim$1.5 V) where the O:Pt ratio progressively increases and place exchange between surface O atoms and Pt can lead to growth of an incipient phase oxide.

Recent sensitive ellipsometric observations in this laboratory have shown that there is no basis for distinction between oxygen species that are detectable by surface coulometry yet are not seen optically by means of ellipsometry. For example, it has been

strongly argued by Bockris and Genshaw[14] (cf.[15]) that the supposed optical distinction of such species indicates an initial chemisorption of O or OH species (detectable only in charging curve experiments) followed by phase oxide formation (which then is optically detectable). Our recent data[16] indicate, however, a close correspondence between the optical signal from the surface and the charge passed in oxidizing it. In sufficiently pure solutions, using the potentiodynamic method, and with sensitive ellipsometry based on off-balance intensity measurements, the optical and electrochemical behavior can be shown to be closely related. Figure 18 (obtained by Dr. Laliberte in this laboratory) illustrates the results obtained and should provide evidence which can settle the disputed[14,15] relation between optical and electrochemical behavior of Pt surfaces. While our present electrochemical results indicate that various states of the oxidized Pt surface can be distinguished, it is important to note that this conclusion evidently cannot be based on the comparison of ellipsometric and electrochemical charging experiments in the initial stages of Pt surface oxidation. Figure 18 does show, however, that at rather higher anodic potentials, there is a real discontinuity in the relation between changes of Δ and changes of charge required for progressive oxidation of the surface. This may be the potential corresponding to onset of phase oxide formation by place exchange since here there is a real change of optical properties of the surface. The discontinuity in the Δ-Q_O/Q_H relation also occurs close to the discontinuity in the relation between Q_O/Q_H and potential, and corresponds to end of the OA2 peak.

Continuing work

Now that the study of the behavior of oxidized Pt surfaces has been studied in considerable detail at room temperature, it is planned to extend the experiments to higher temperatures by means of the technique that has been built up in parallel with the work reported above, i.e. the employment of the cell in a high temperature bomb together with the in situ H_2 reference electrode system recently developed and described above.

Reversibility, distinction of various states of surface oxidation of the electrodes, etc. will be investigated at elevated temperature with Pt electrodes and then with Rh and Ir. The relation between the initial stages of noble metal surface oxidation and intermediates in the O_2 reduction reaction will be examined.

Parallel theoretical work is in progress with regard to computer simulation (cf. ref.[3]) of the oxidation curves at Pt for room temperature in relation to the single cathodic reduction peak that is usually observed in the cathodic direction of sweep. The principal question here is whether this peak arises from rearrangement of the surface oxide initially laid down (intrinsic hysteresis) or whether it arises kinetically because of a rate-controlling mechanism in reduction which is different from that in oxidation of the surface. This is possible for a highly irreversible reaction and, under these conditions, would not contravene the principle of microscopic reversibility. Thus, in a two-stage oxidation process with the first step at quasi-equilibrium and the second step rate-controlling, the kinetic behavior will be different from that when the reaction is reversed since there would then be no quasi-equilibrium process prior to the rate-controlling step.

Current theoretical work on this project is addressed to investigation of the consequences of considering the oxidation of the surface lattice in terms of building up sub-lattices of OH and O species on the Pt surface depending on the coordination of the OH and O species, e.g. in groups of 4 Pt per OH, 2 Pt per OH, 2 Pt per O etc. It seems that the structure in the differential charging curve, viz. the appearance of peaks in the voltammetric curve, can be explained by means of this approach. The recognition of sub-lattices in the ad-layer is also consistent with LEED observations on O adsorption at low and intermediate coverages at various metals, e.g. Ni, from the gas phase.

Finally, work is in progress on the surface oxidation of the 110, 100 and 111 single crystal faces of Pt in order to establish how the structure of the oxidation curves depends on the atomic spacing and arrangement, in relation to sub-lattice formation in the ad-layer of OH and O species.

References

1. Conway, J. Electroanal. Chem. 8, 486 (1964).
2. Gileadi and Srinivasan, Electrochim. Acta, 11, 321 (1966).
3. Stonehart, Kozlowska and Conway, Proc. Roy. Soc. London. A310 541 (1969).
4. E. g. Schuldiner and Warner, J. Phys. Chem. 68, 1223 (1964).
5. Kozlowska and Conway, J. Electroanal. Chem. 7, 109 (1964).
6. Brief reports to N. A. S. A. on Grant No. N. G. R. 52-093-001 dated September 1970 and October 1969.
7. MacDonald and Conway, Proc. Roy. Soc. London, A269, 419 (1962).
8. Giner, J. Electrochem. Soc., 111, 376 (1964).
9. Gilroy and Conway, Can. J. Chem. 46, 875 (1968).
10. Gilroy and Conway, J. Phys. Chem. 69, 1259 (1965).
11. Vielstich, Brennstoffelemente, Springer Verlag.
12. Conway, Gilroy and Sattar, Electrochim. Acta, 14, 711 (1969).
13. Urbach et al, J. Electrochem. Soc., 117, 1500 (1970).
14. Reddy, Genshaw and Bockris, J. Electroanal. Chem., 8, 406 (1964; Chem. Phys. 48, 671 (1968).
15. Greef, J. Chem. Phys. 51, 3148 (1969).
16. Conway and Laliberte, Faraday Society Symposium on Optical Studies of Surface Layers, December 1970 (Discussion remarks).

Figure 1

Effect of temperature on behavior of Giner type reference electrode.

364°K	298°K	
△	X	H_2 bubbled through reference cell
□	O	H_2 not bubbled (this work)
■	●	H_2 not bubbled (Giner's data)

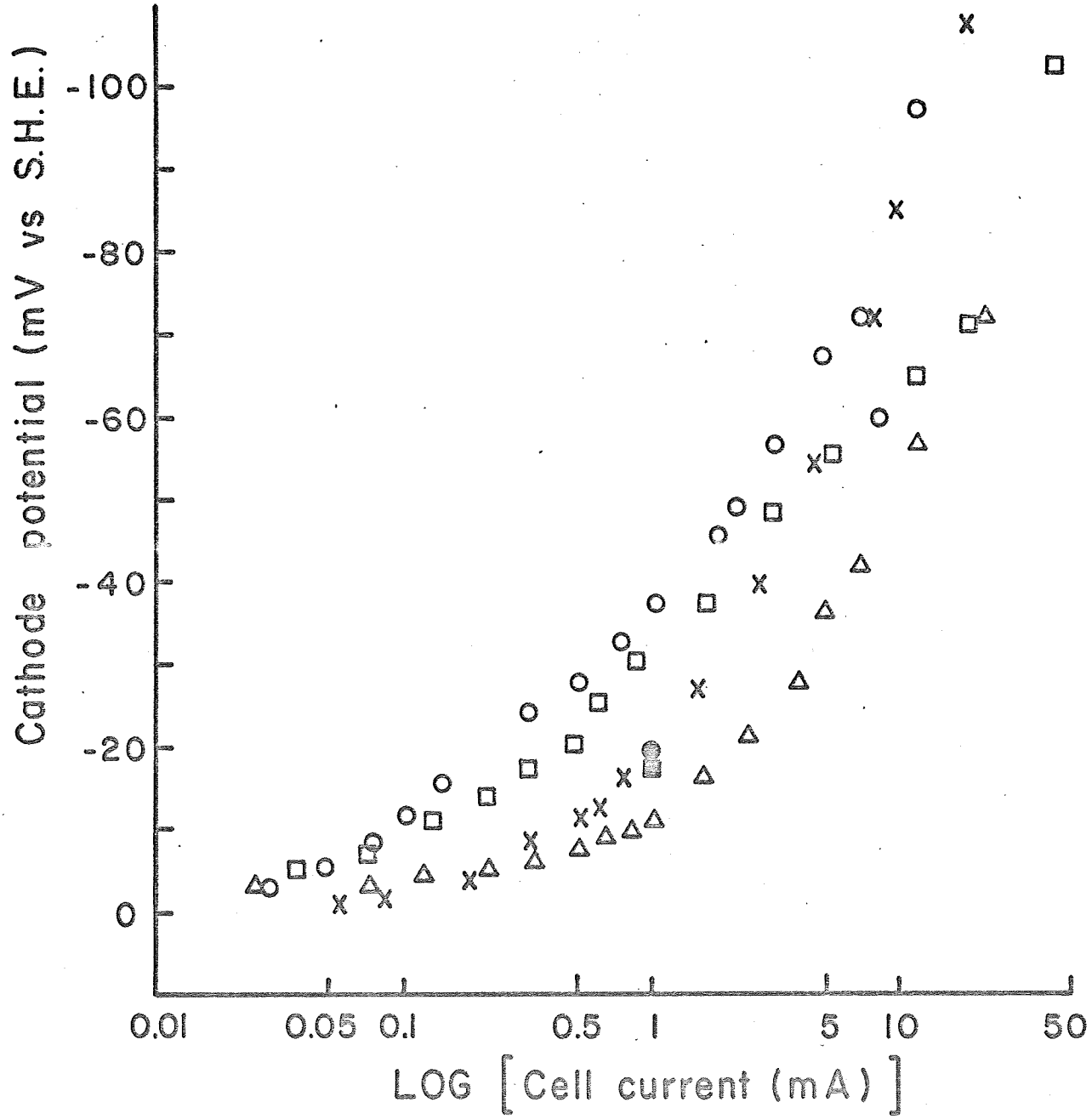
Cathode potential (mV vs S.H.E.)
-100
-80
-60
-40
-20
0
0.01
0.05
0.1
0.5
1
5
10
50
LOG [Cell current (mA)]

Figure 2

Effect of diffusing oxygen on potential of Giner type reference cathode at room temperature

Anode and cathode in same compartment	Anode and cathode separated	
O	□	H_2 bubbled
X	Δ	H_2 not bubbled (this work)
■		Hydrogen not bubbled (Giner's result)

(Points on left-hand side are not steady values)

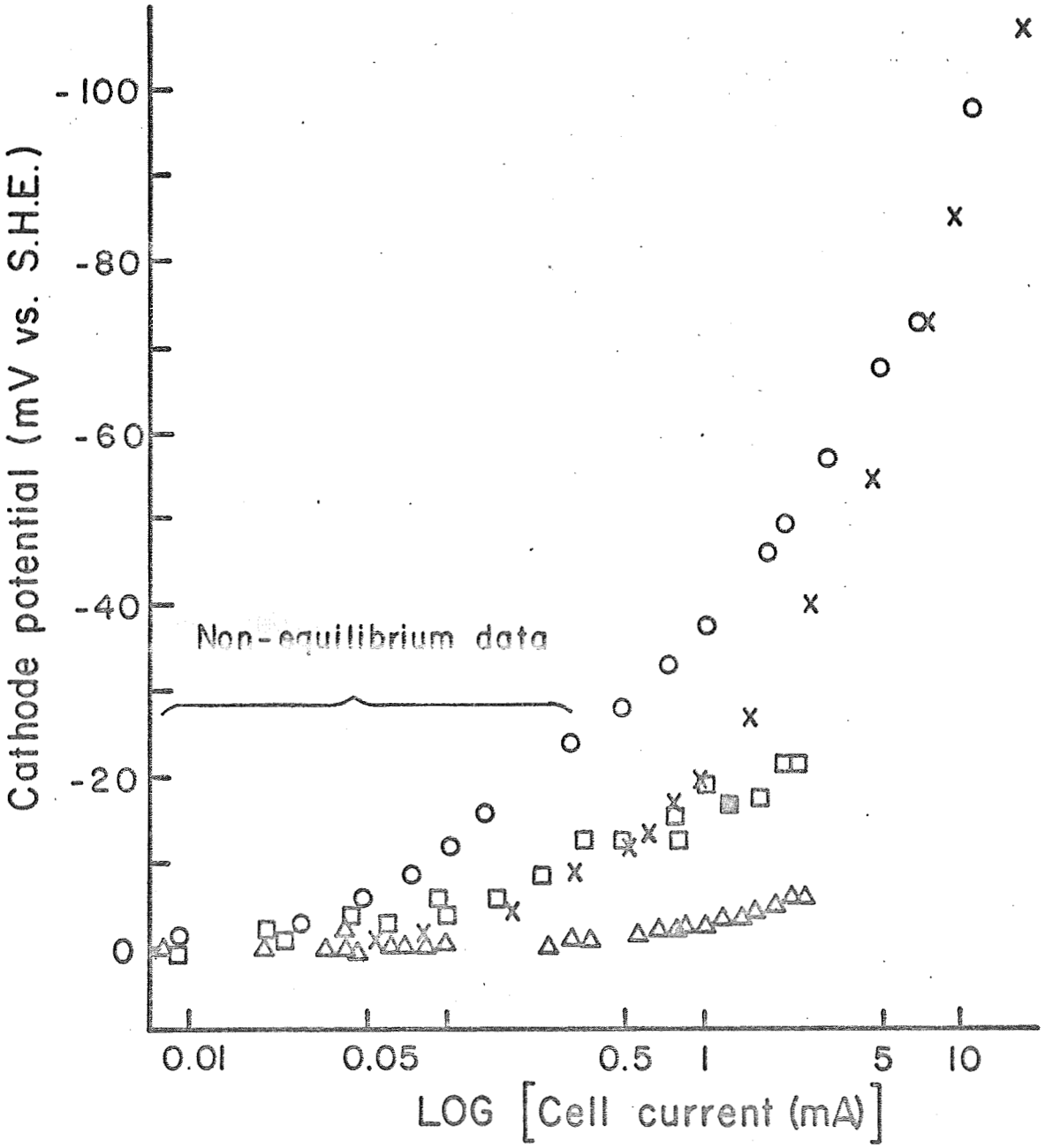
Cathode potential (mV vs. S.H.E.)
-100
-80
-60
-40
-20
0
Non-equilibrium data
0.01
0.05
0.5
1
5
10
LOG [Cell current (mA)]

Figure 3

Effect of temperature on potential of the new three electrode reference system

● Points for 302°K

I Band for spread of potential data at 368°K. (Points to the left are unsteady values)

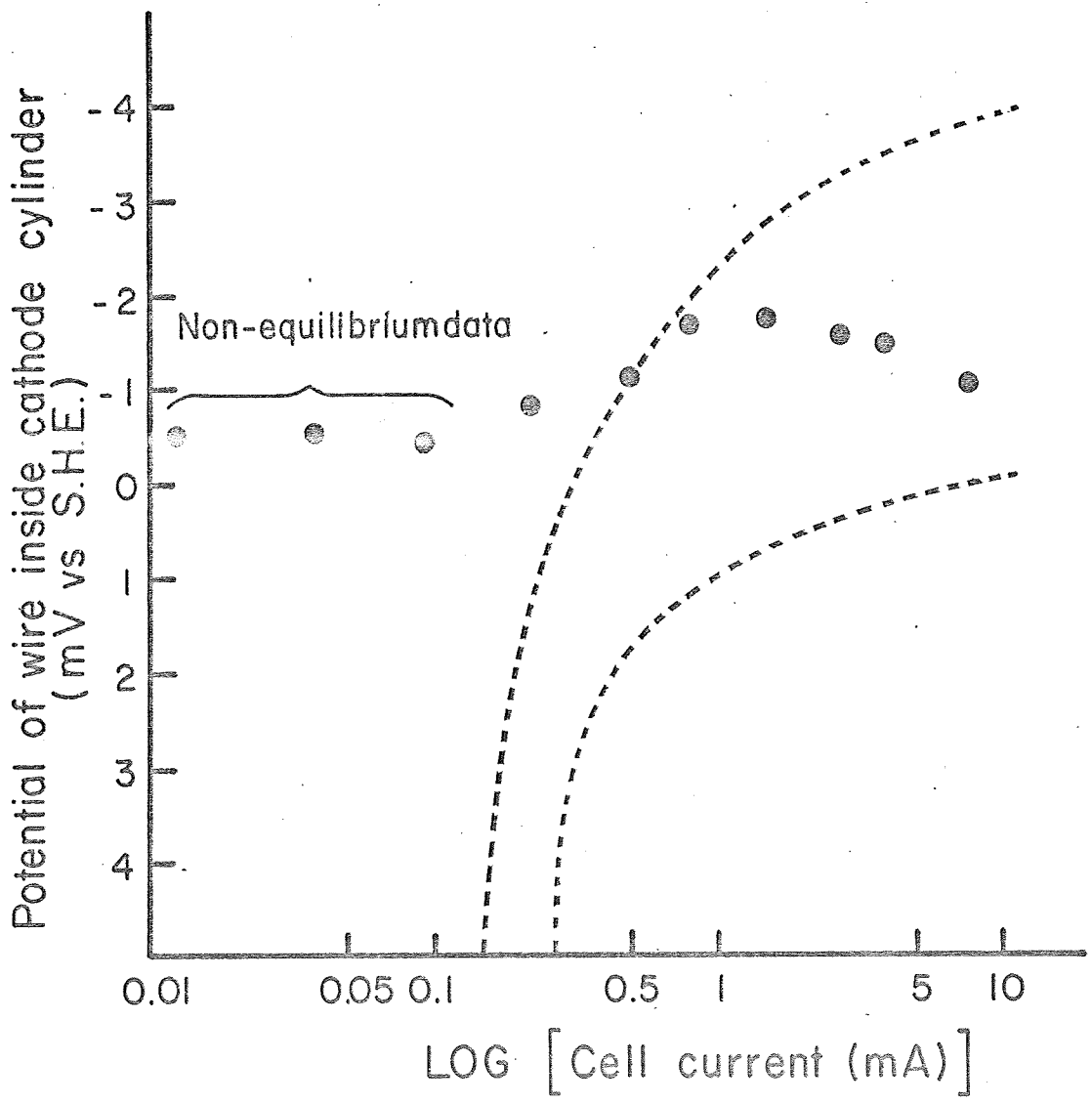
Potential of wire inside cathode cylinder (mV vs S.H.E.)
-4
-3
-2
-1
0
1
2
3
4
Non-equilibrium data
0.01
0.05
0.1
0.5
1
5
10
LOG [Cell current (mA)]

Figure 4

Pt surface oxidation behavior over a range of temperatures

(1N H_2SO_4)

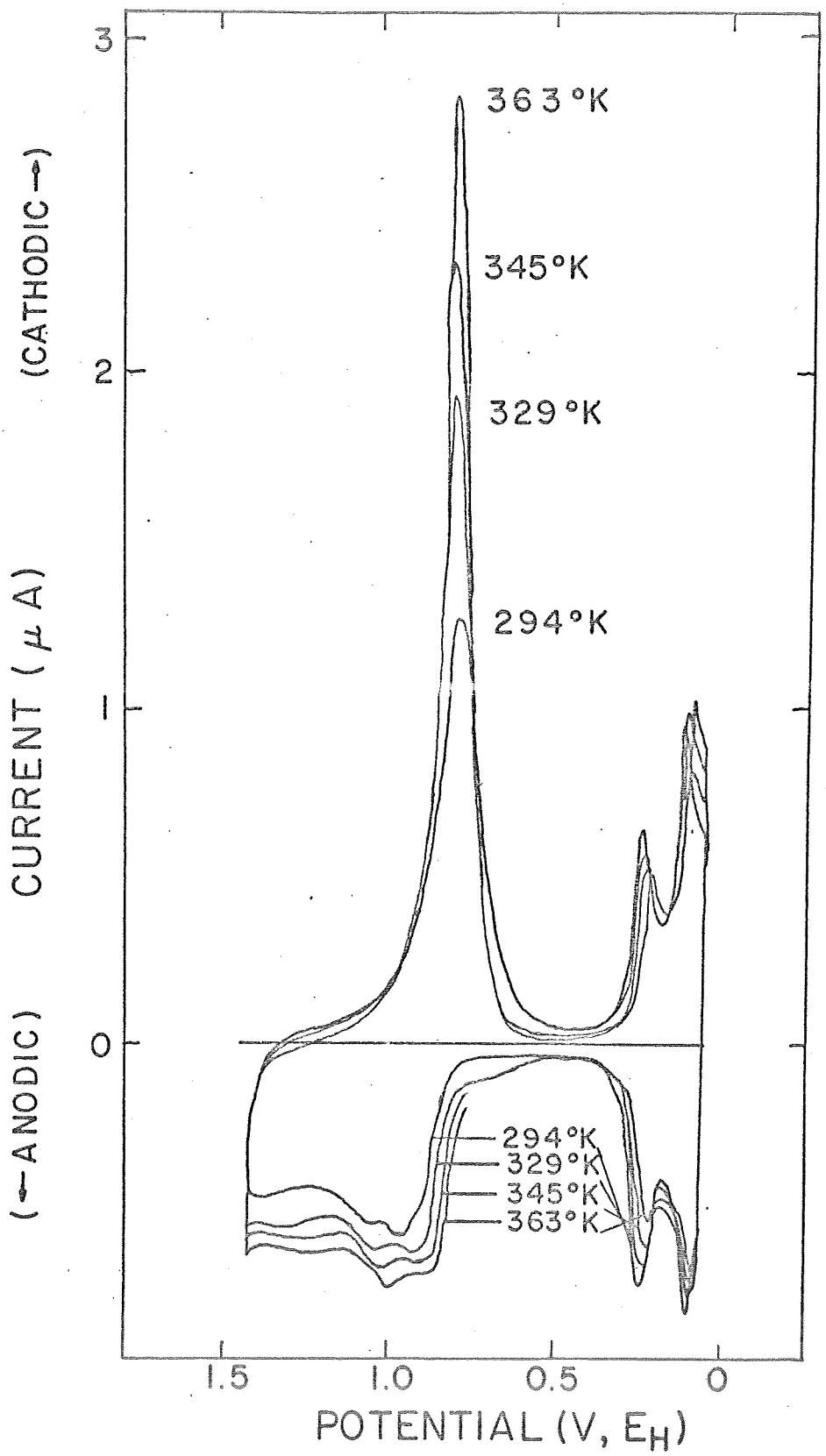
363°K
345°K
329°K
294°K
294°K
329°K
345°K
363°K
3
2
1
0
1.5
1.0
0.5
0
(—ANODIC) CURRENT (μA) (CATHODIC→)
POTENTIAL (V, E_H)

Figure 5

Comparison of potentiodynamic surface oxidation and reduction behavior of Pt in 1 N H_2SO_4 and 1 N $HClO_4$. (Note slightly different reduction of current profiles in the anodic direction of potential sweep)

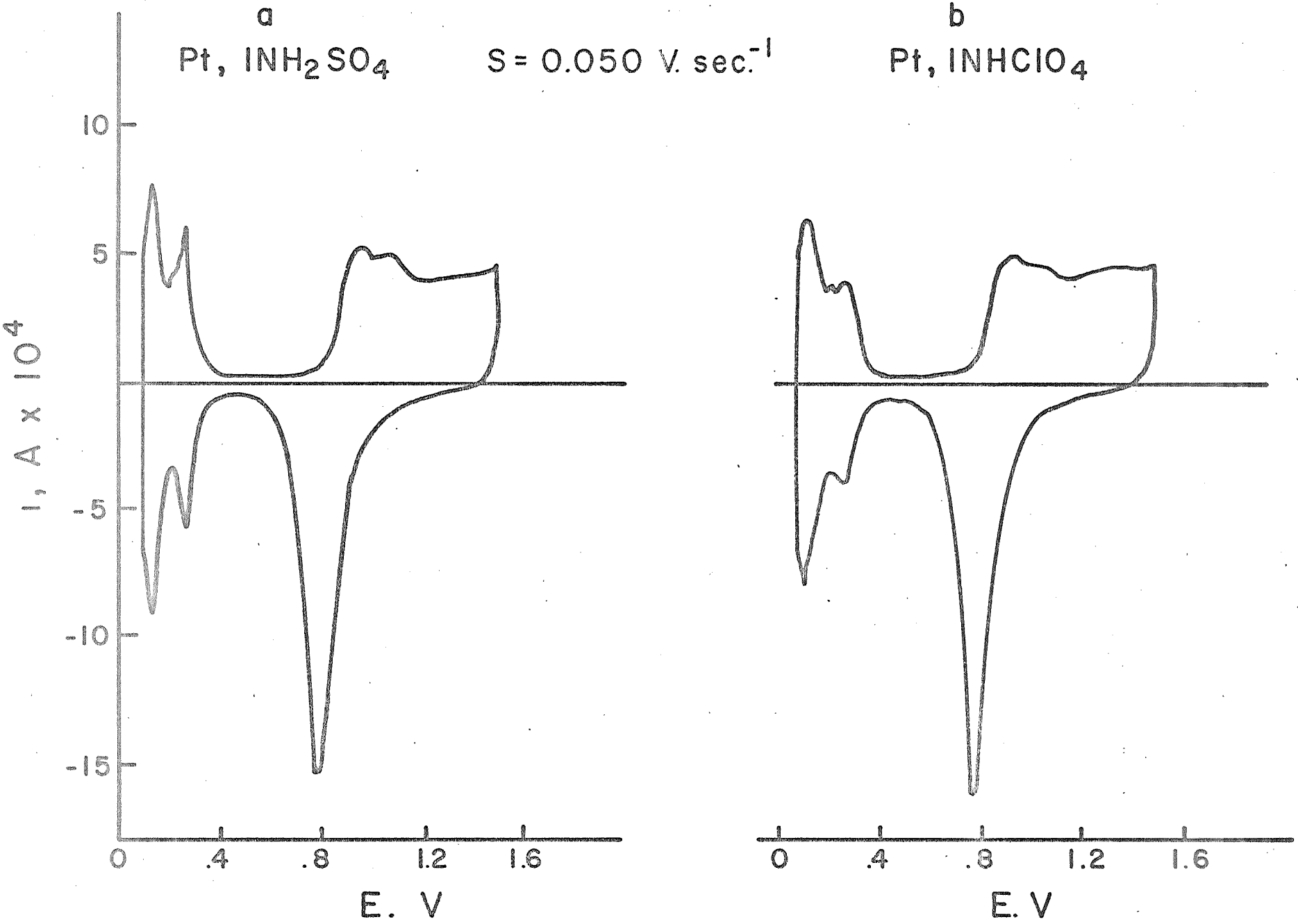
a
Pt, INH_2SO_4
S = 0.050 V. $sec.^{-1}$
b
Pt, $INHClO_4$
10
5
-5
-10
-15
I, A x 10^4
0
.4
.8
1.2
1.6
E. V
0
.4
.8
1.2
1.6
E. V

Figure 6

Potentiodynamic current-potential profile for surface oxidation and reduction at platinized Pt indicating the various regions of H oxidation, surface oxide formation and reduction and H re-deposition. (1 M H_2SO_4, 25°C, sweep rate = 0.1 V. sec^{-1})

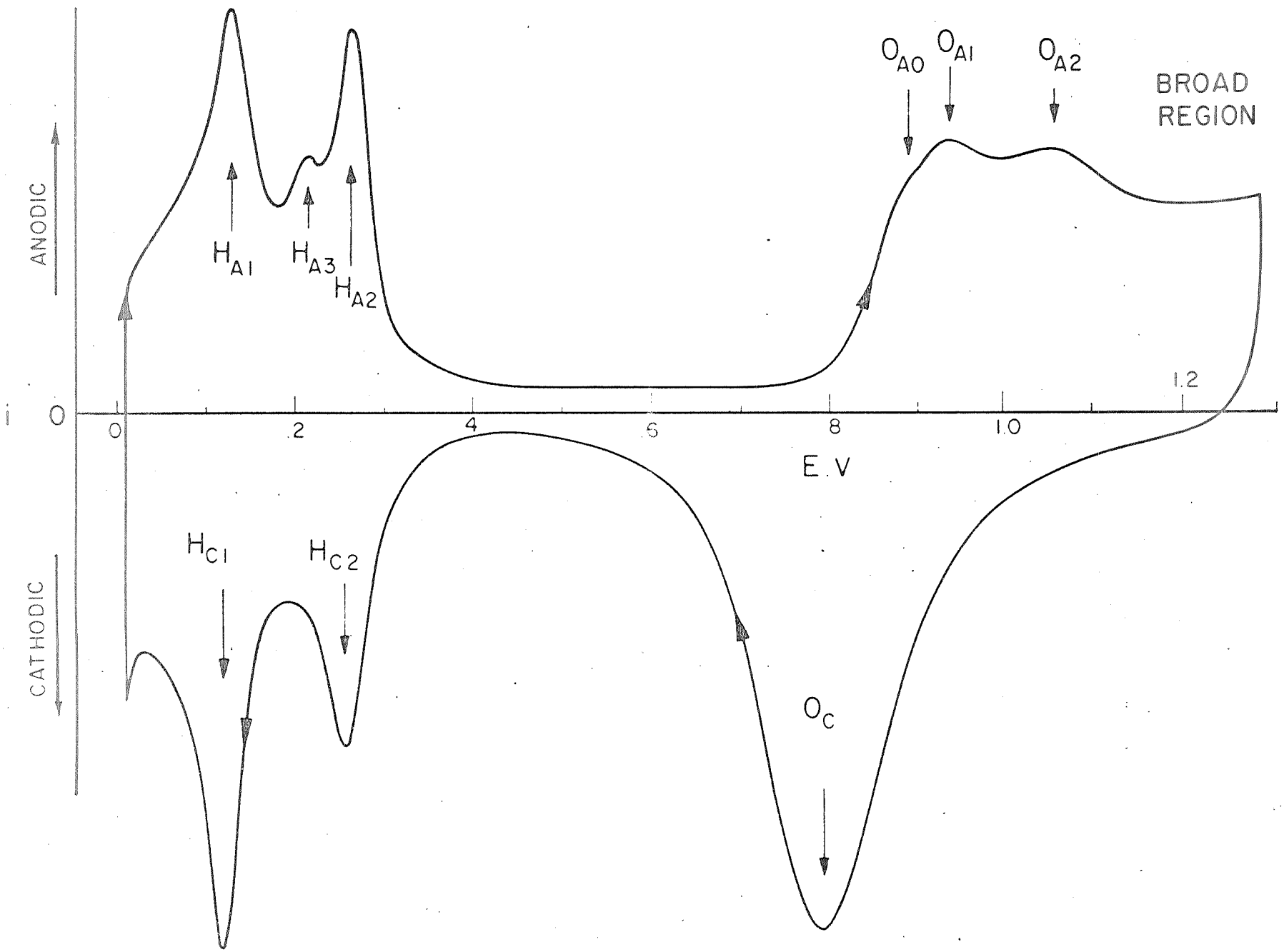
ANODIC
CATHODIC
i
0
H_{A1}
H_{A3}
H_{A2}
O_{A0}
O_{A1}
O_{A2}
BROAD REGION
0
.2
.4
.6
.8
1.0
1.2
E.V
H_{C1}
H_{C2}
O_C

Figure 7

Porentiodynamic current-potential profiles for surface oxidation of Pt and for Faradaic oxidation of HCOOH on the same electrode showing relation between the regions of oxidation of HCOOH and the state of oxidation of the Pt surface. Scale for HCOOH currents is 10 x smaller than for surface oxidation currents.

---------- 1 M aq. H_2SO_4

———————— 1 M aq. H_2SO_4 + 0.5 M HCOOH

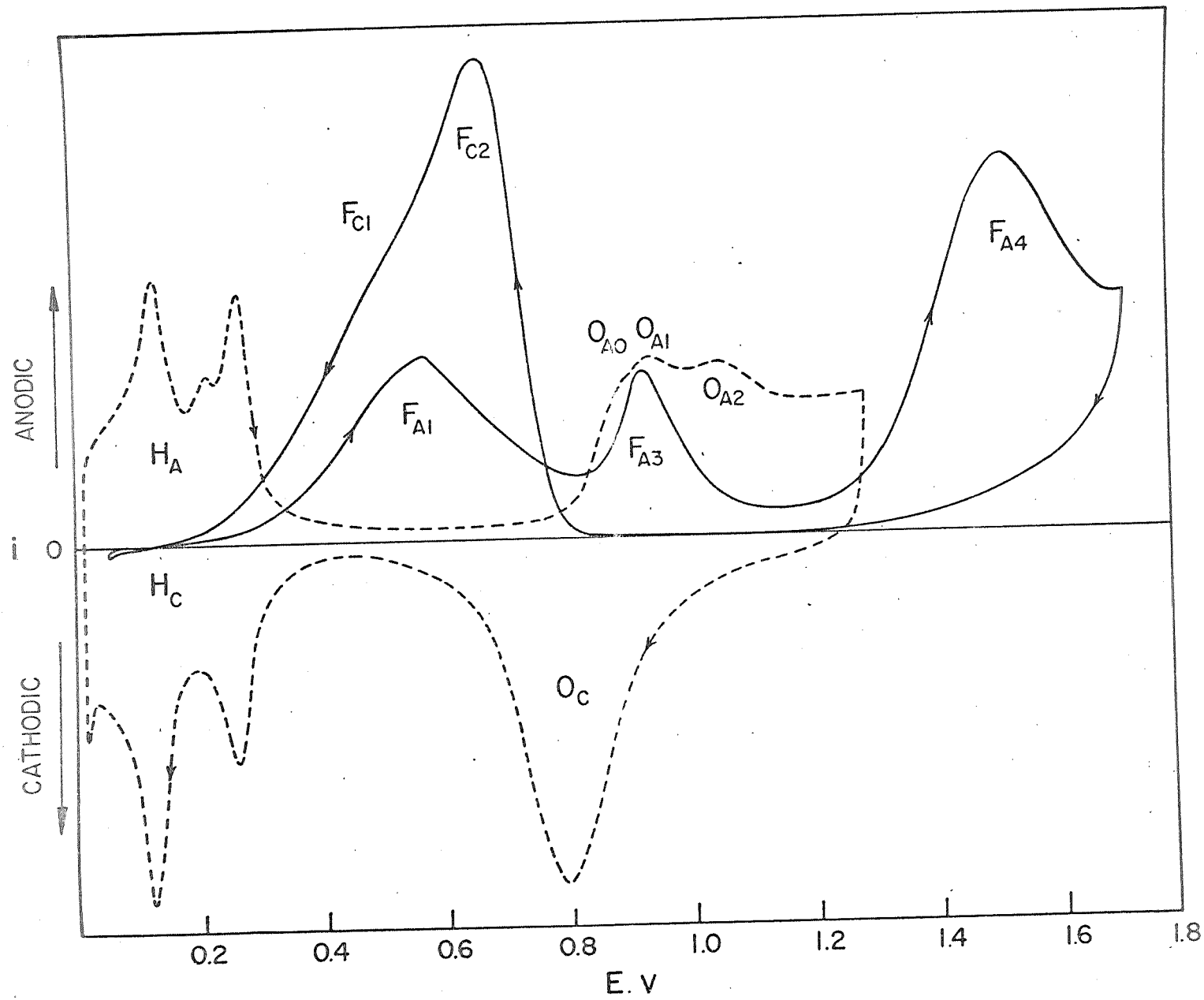
ANODIC
i
0
CATHODIC
F_{C1}
F_{C2}
F_{A1}
F_{A3}
F_{A4}
O_{A0}
O_{A1}
O_{A2}
H_A
H_C
O_C
0.2
0.4
0.6
0.8
1.0
1.2
1.4
1.6
1.8
E. V

Figure 8

Effects of acetonitrile on potentiodynamcc current-potential profile for surface oxidation of Pt (s = 0.10 V. sec^{-1}; 1 N aq. H_2SO_4)

----- zero concentration of CH_3CN

..... 2×10^{-5} M CH_3CN

——— 3×10^{-3} M CH_3CN

-.-.- 3×10^{-2} M CH_3CN

(Note: effects of CH_3CN are similar to those of typical impurities in unpurified solutions)

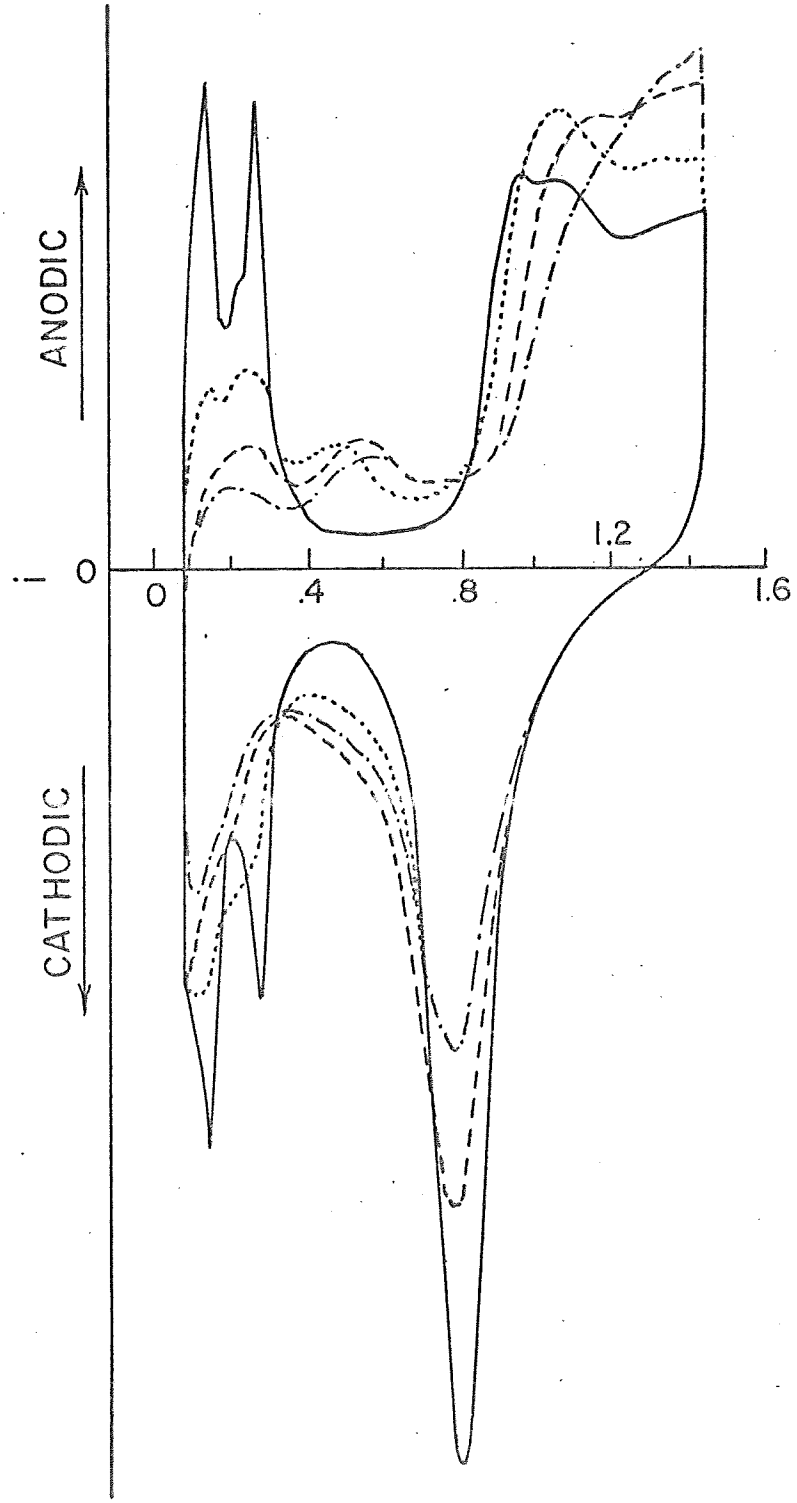
ANODIC
CATHODIC
i
0
0
.4
.8
1.2
1.6

Figure 9

Potentiodynamic current-potential profiles for formation and reduction of surface oxide species on platinized Pt in 1 M aq. H_2SO_4 from 0.45 V (E_H) to various anodic termination potentials E_A. $s = 0.10\ V.sec^{-1}$. Also shown is integral charge for surface oxidation expressed as the ratio Q_O/Q_H as a function of potential.

Note changing degree of reversibility of formation and reduction processes with increasing E_A and inflection in Q_O/Q_H ratio at E = 1.12 V.

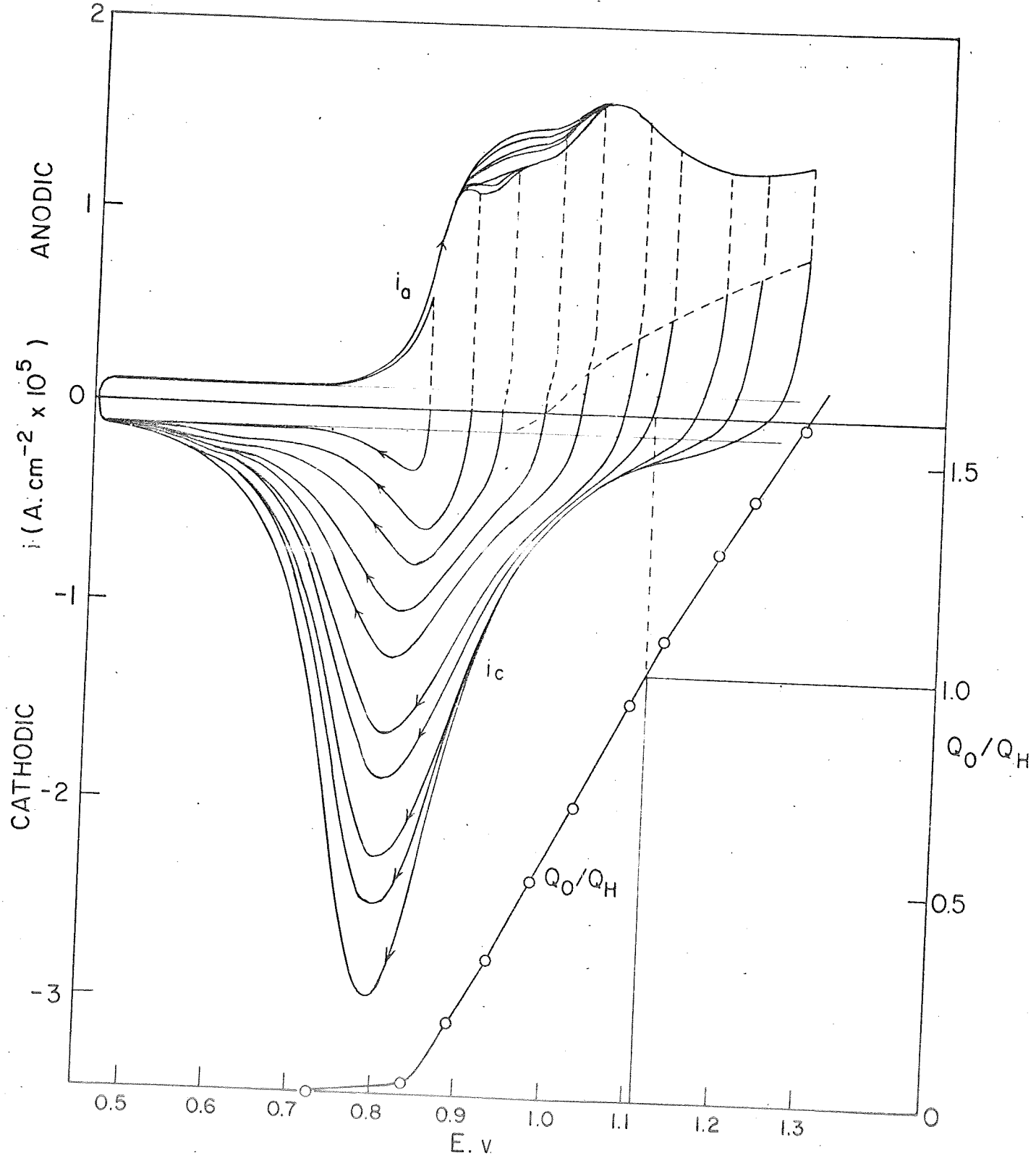
2
1
0
-1
-2
-3
ANODIC
CATHODIC
i (A. cm⁻² x 10⁵)
i_a
i_c
Q_O/Q_H
1.5
1.0
0.5
0
0.5
0.6
0.7
0.8
0.9
1.0
1.1
1.2
1.3
E. V

Figure 10

Dependence of cathodic peak potential $E_{p,c}$ on extent of surface oxidation Q_O/Q_H and on corresponding potential .

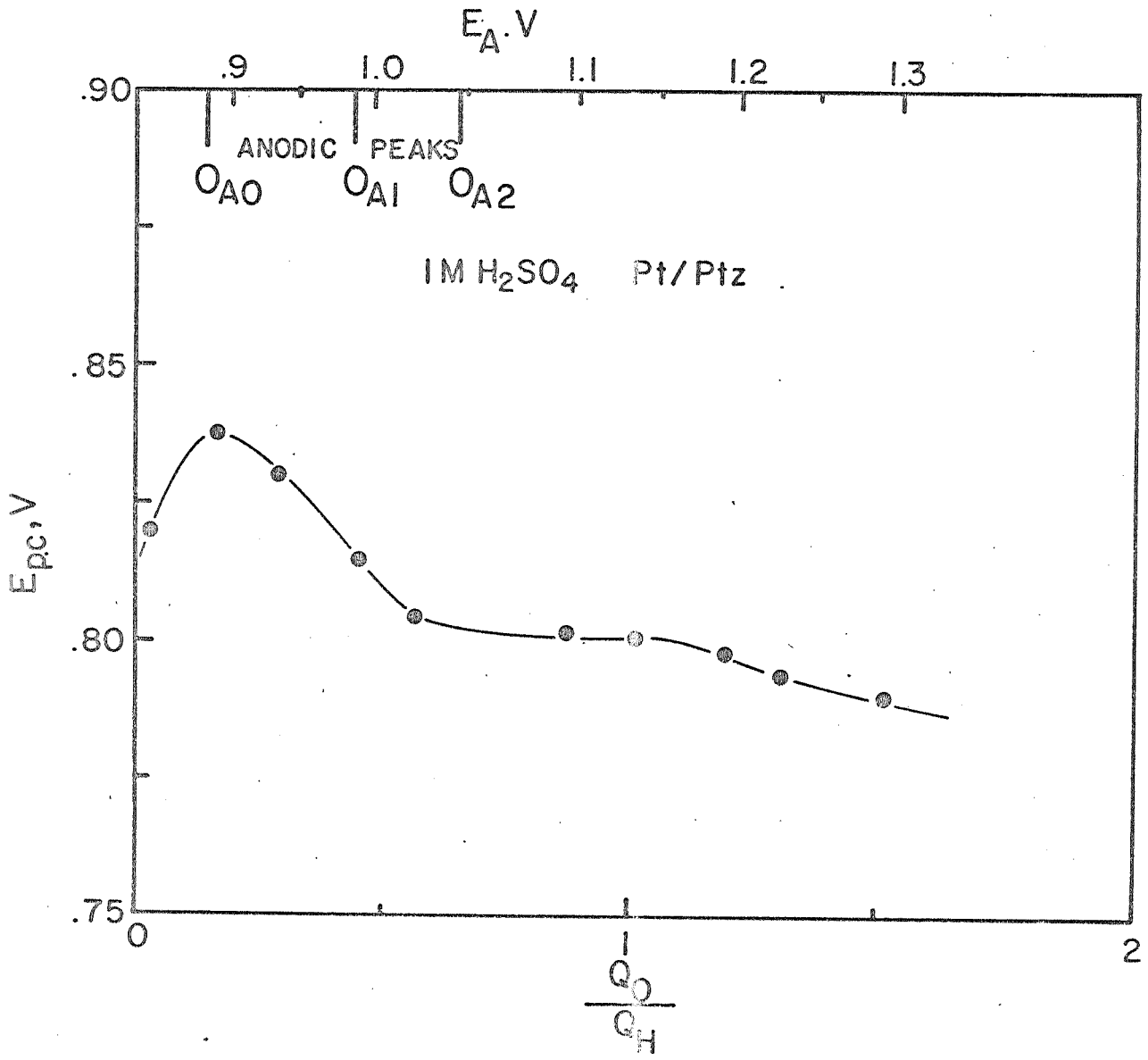
E_A, V
.9
1.0
1.1
1.2
1.3
.90
.85
.80
.75
ANODIC PEAKS
O_{A0}
O_{A1}
O_{A2}
1M H_2SO_4 Pt/Ptz
E_{pc}, V
0
1
2
$\frac{Q_O}{Q_H}$

Figure 11

Relation between cathodic peak potential on sweep rate s for reduction of surface oxides at Pt formed up to various anodic termination potentials E_A

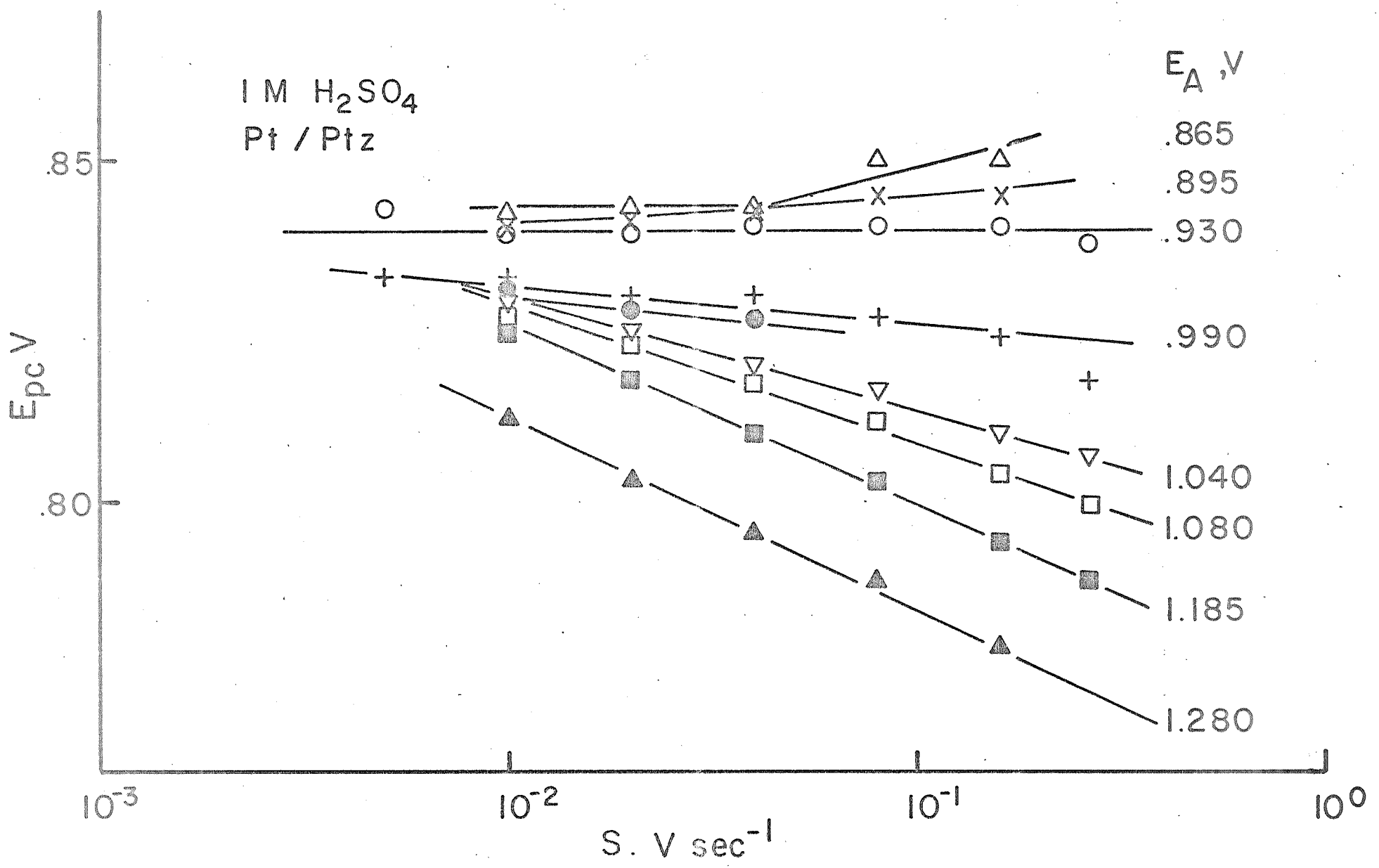
1 M H_2SO_4
Pt / Ptz
E_A ,V
.865
.895
.930
.990
1.040
1.080
1.185
1.280
.85
.80
E_{pc} V
10^{-3}
10^{-2}
10^{-1}
10^{0}
S. V sec^{-1}

Figure 12

Tafel slopes expressed as $d \cdot E_{p,c}/d \log s$ for reduction of Pt surface oxide formed at various anodic termination potentials.

⊙ multisweeps up to various E_A

X from reduction sweep after anodic holding at E_A = 1.19 V for 1 min.

\+ from reduction sweep after anodic holding at E_A = 1.45 V for 20 min.

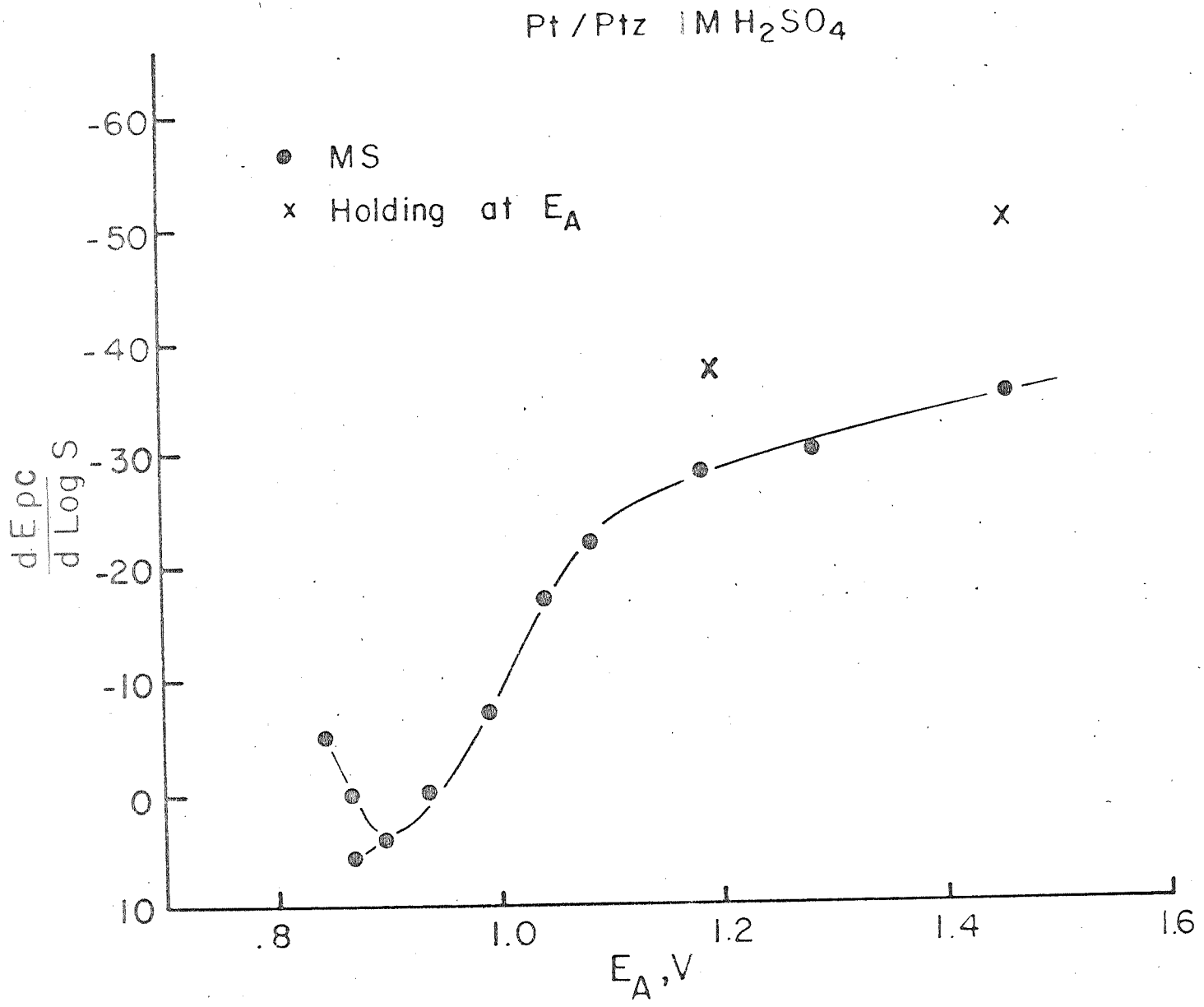
Pt / Ptz 1M H_2SO_4
MS
Holding at E_A
-60
-50
-40
-30
-20
-10
0
10
$\frac{dE_{pc}}{d\,Log\,S}$
.8
1.0
1.2
1.4
1.6
E_A, V

Figure 13

Tafel slopes expressed as $d E_{p,c}/d \log s_c$ for cathodic sweeps at various rates s_c but for constant anodic sweep rate $s_a \approx 1.0$ V. sec^{-1}.

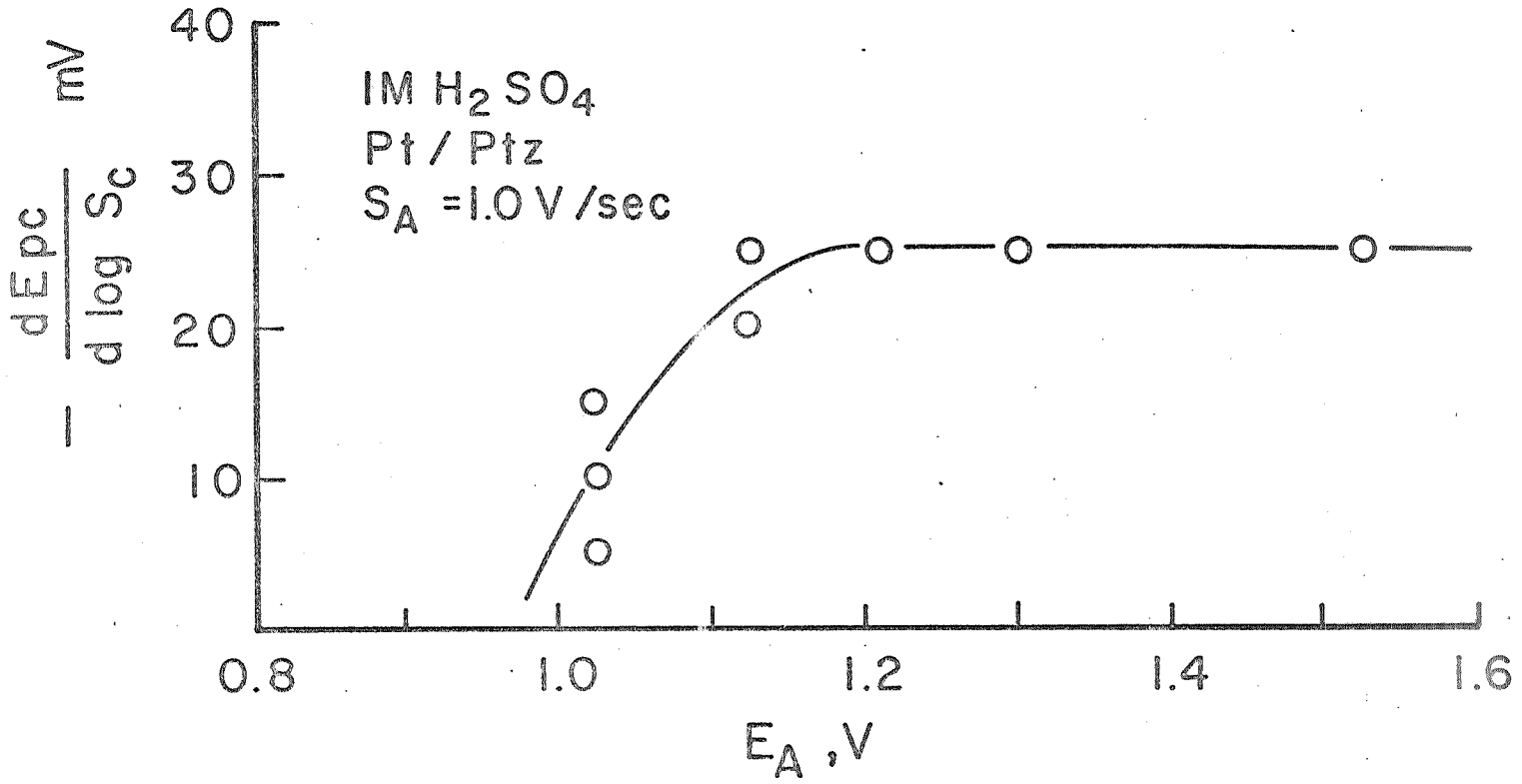
40
30
20
10
mV
dEpc / d log Sc
1M H2 SO4
Pt / Ptz
SA = 1.0 V/sec
0.8
1.0
1.2
1.4
1.6
EA , V

Figure 14 (a)

Current-potential profiles for multisweeps at platinized Pt over progressively shorter ranges of potential. In curve h, oxidation-reduction current envelope progressively diminishes with time of cycling.

(b)

As in 14a but for progressively changing cathodic termination potentials in multisweep experiments.

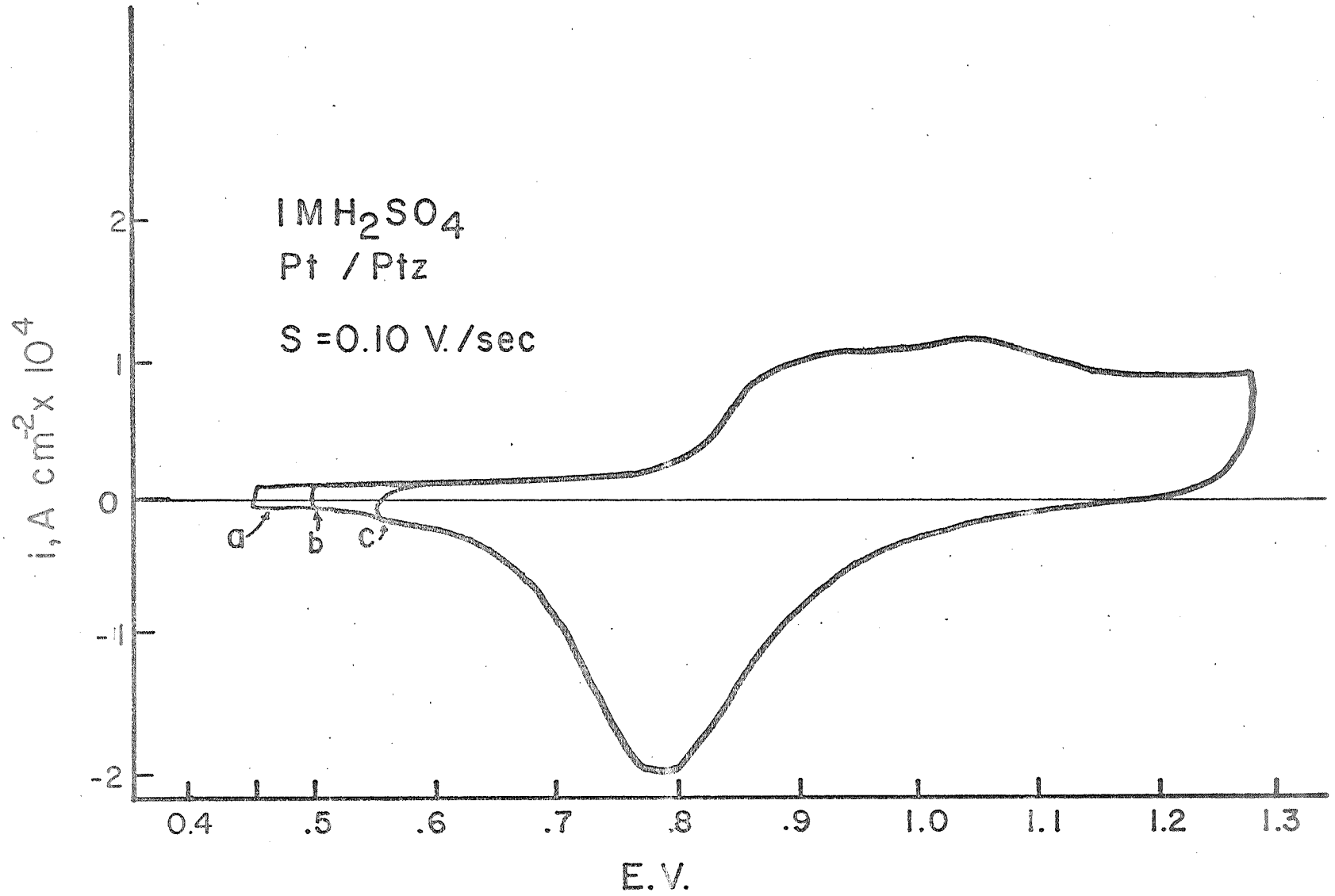
1 M H2SO4
Pt / Ptz
S = 0.10 V./sec
i, A cm-2 x 10^4
2
1
0
-1
-2
a
b
c'
0.4
.5
.6
.7
.8
.9
1.0
1.1
1.2
1.3
E. V.

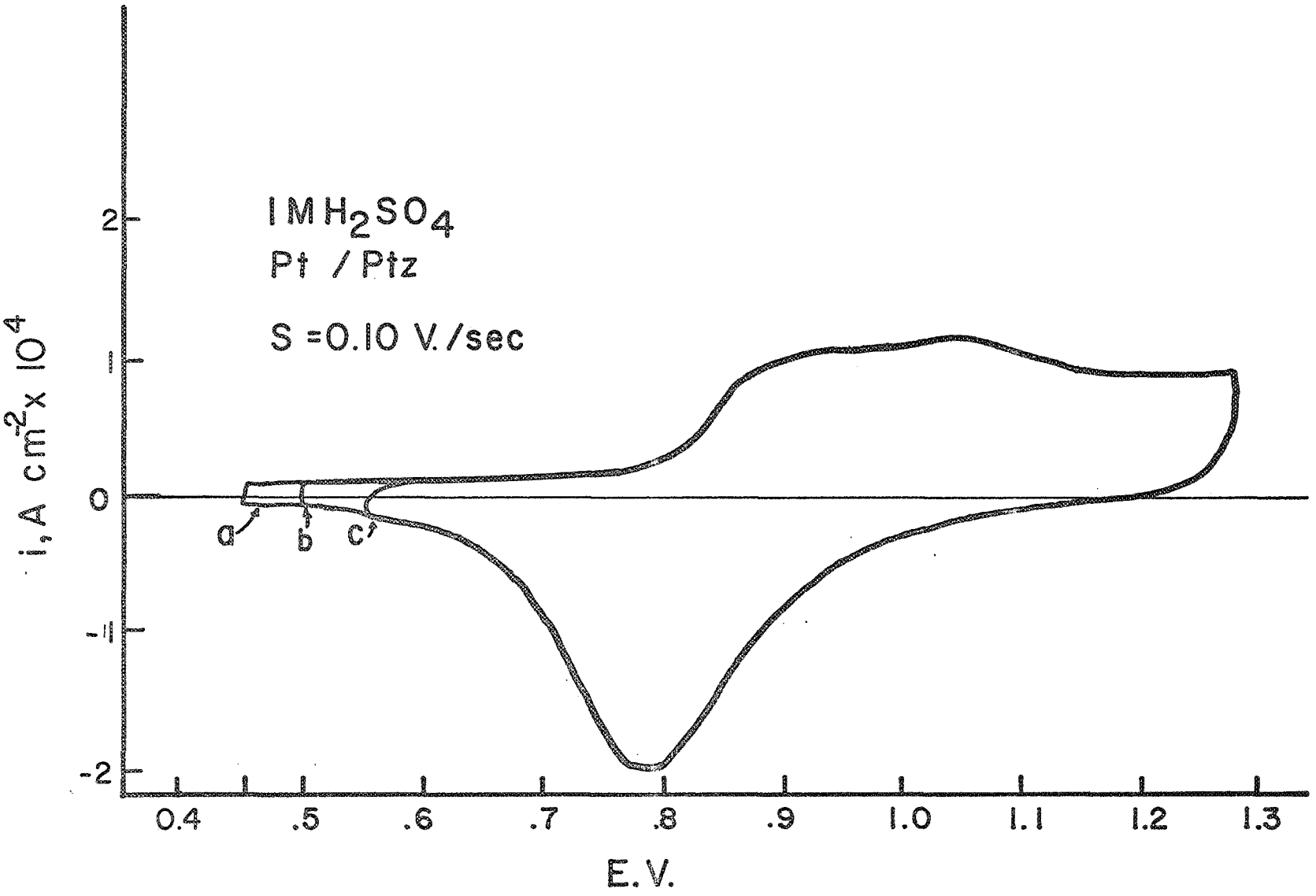
1 M H2SO4
Pt / Ptz
S = 0.10 V./sec
i, A cm-2 x 10^4
2
0
-2
a
b
c
0.4
.5
.6
.7
.8
.9
1.0
1.1
1.2
1.3
E. V.

Figure 15

(a)

Time effects in cathodic sweeps for reduction of surface oxide at platinised Pt after various periods of anodic holding at E_A = 0.89 V (s = 0.10 V. sec^{-1}). Curve a, multisweep; b, 0.5 m; c, 1 m; d 5 m ; e, 10 m; f, 30 m. holding time.

(b)

As in 15a but for anodic hdding at E_A = 0.94 V (s = 0.10 V. sec^{-1}). Curve a, multisweep; b, 0.5 m; c, 1 m; d, 5 m; e, 10 m; f, 30 m. holding time.

(c)

As in 15a but for anodic holding at E_A = 1.0 V (s = 0.10 V. sec^{-1}). Curve a, multisweep; b, 0.5 m; c, 1. m; d, 5m; e, 10 m. holding time.

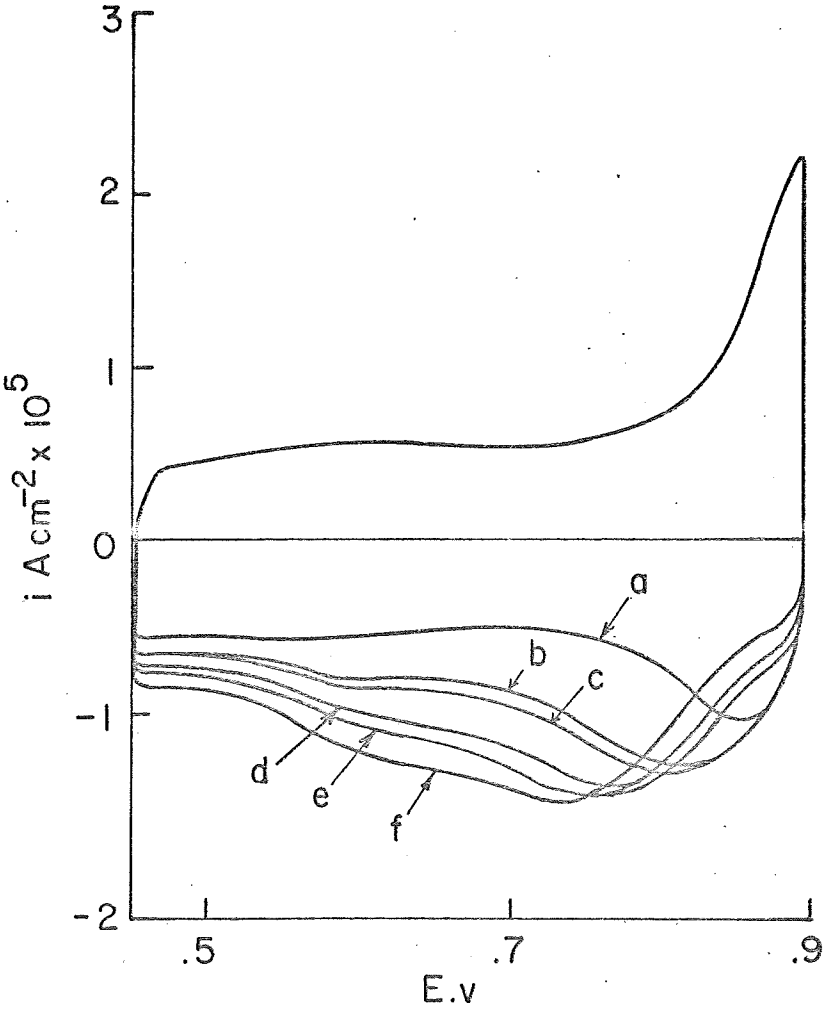
3
2
1
0
-1
-2
i A cm^{-2} x 10^5
a
b
c
d
e
f
.5
.7
.9
E.v

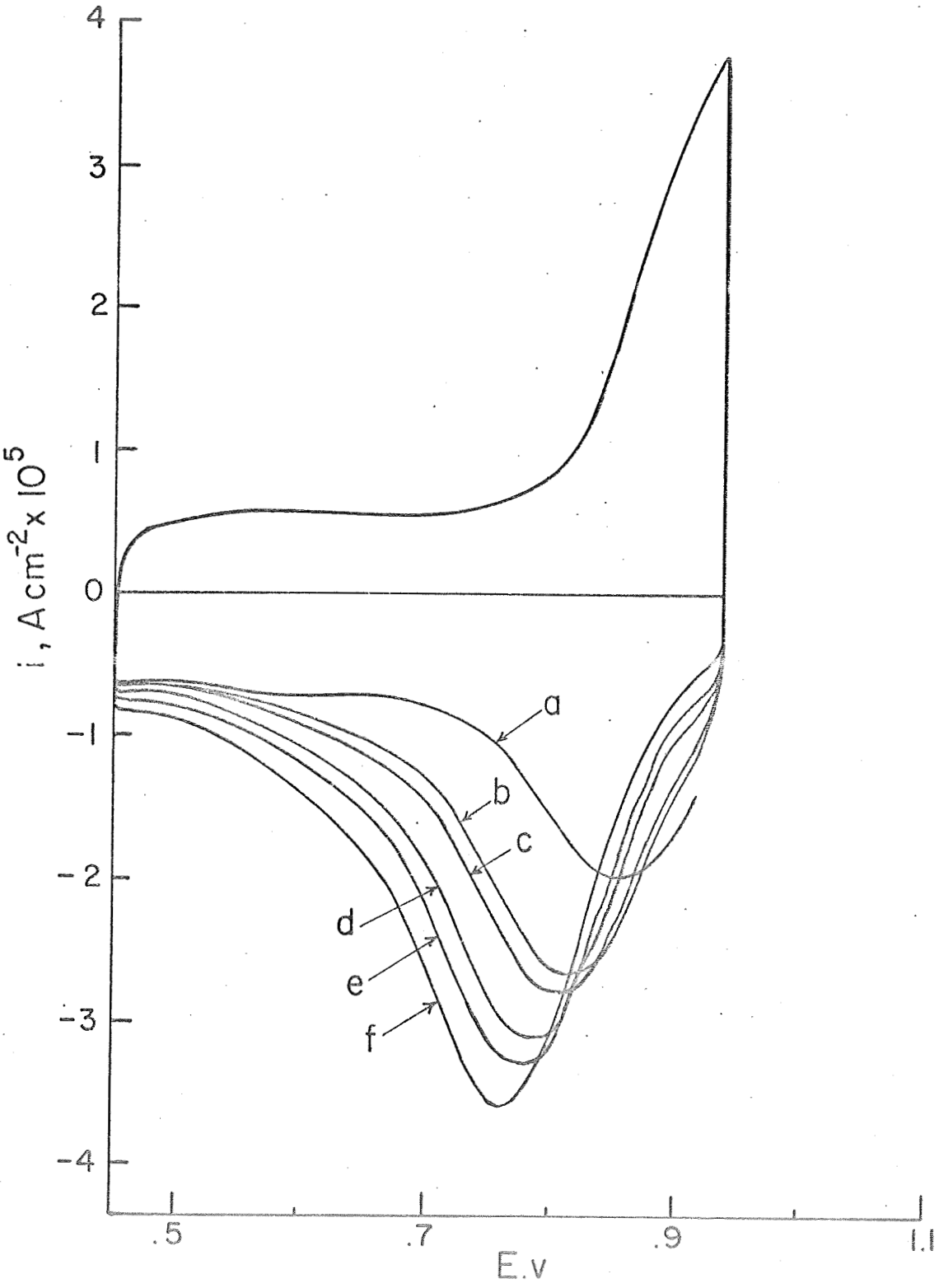
4
3
2
1
0
-1
-2
-3
-4
i, A cm^{-2} x 10^5
a
b
c
d
e
f
.5
.7
.9
1.1
E.v

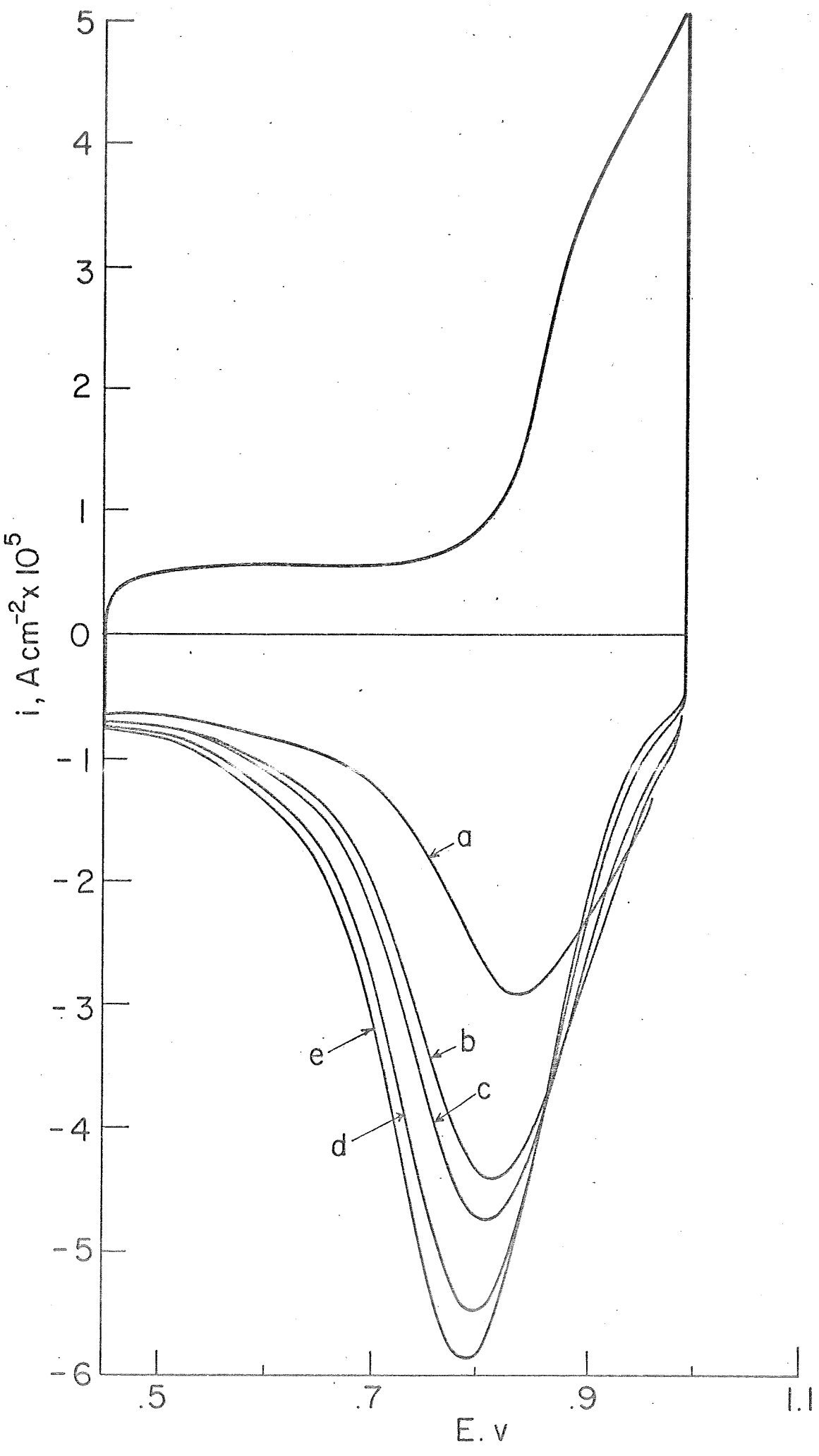
5
4
3
2
1
0
-1
-2
-3
-4
-5
-6
i, A cm^{-2} x 10^5
.5
.7
.9
1.1
E. v
a
b
c
d
e

Figure 16

Relation between cathodic peak potential $E_{p,c}$ and degree of surface oxidation Q_O/Q_H for surface oxide formed at various anodic termination potentials E_A for various periods of anodic holding as in Figs. 15a-c.

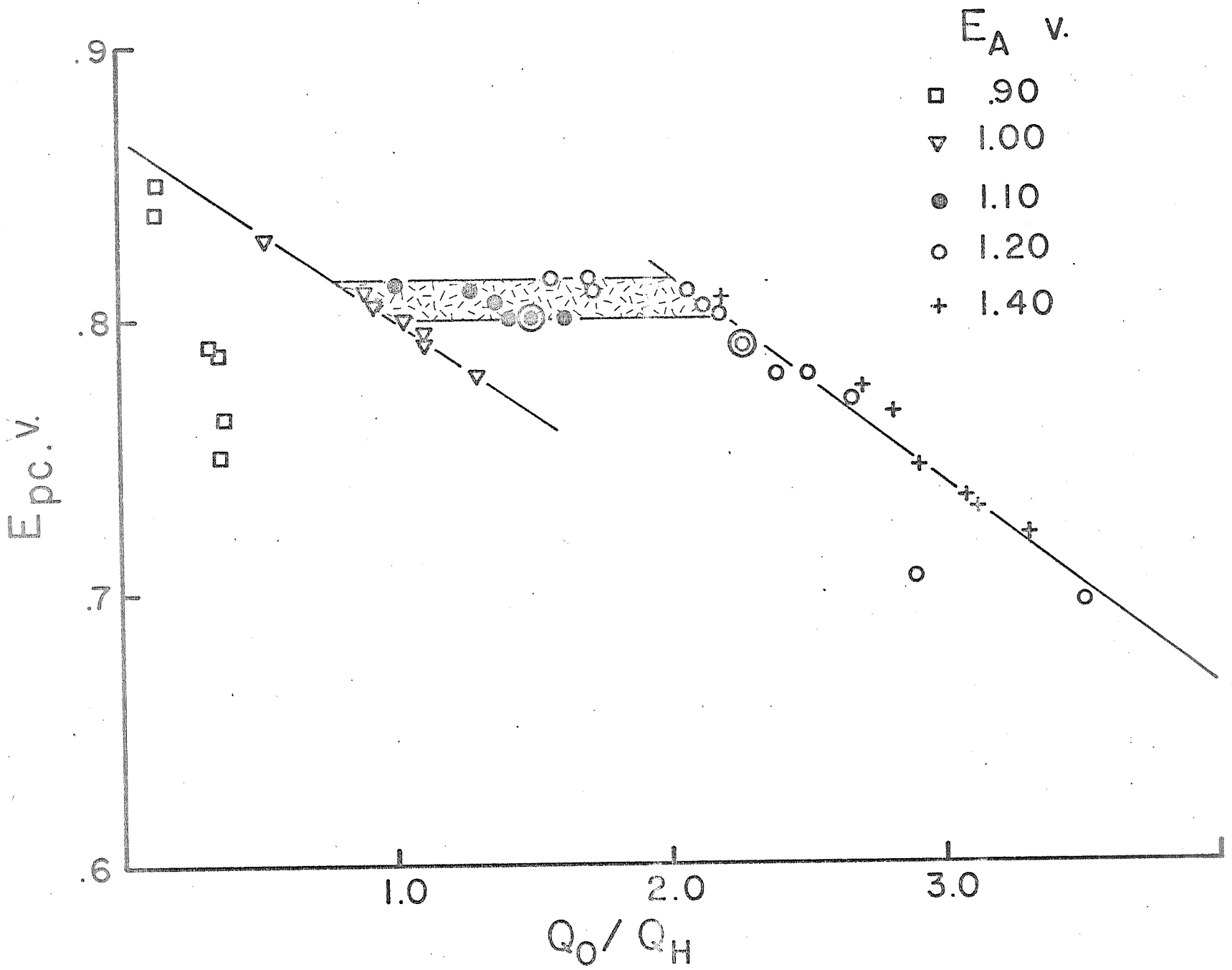
E_A v.
.90
1.00
1.10
1.20
1.40
.9
.8
.7
.6
E_{pc} v.
1.0
2.0
3.0
Q_O / Q_H

Figure 17

Comparison of potential dependence of integral charges for surface oxidation of platinized platinum in 1 M KOH and 1 M H_2SO_4 at 25°C. Relation of peak potentials for acid and alkaline solutions is shown on upper scales.

X Data for KOH solutions

O Data for H_2SO_4 solutions

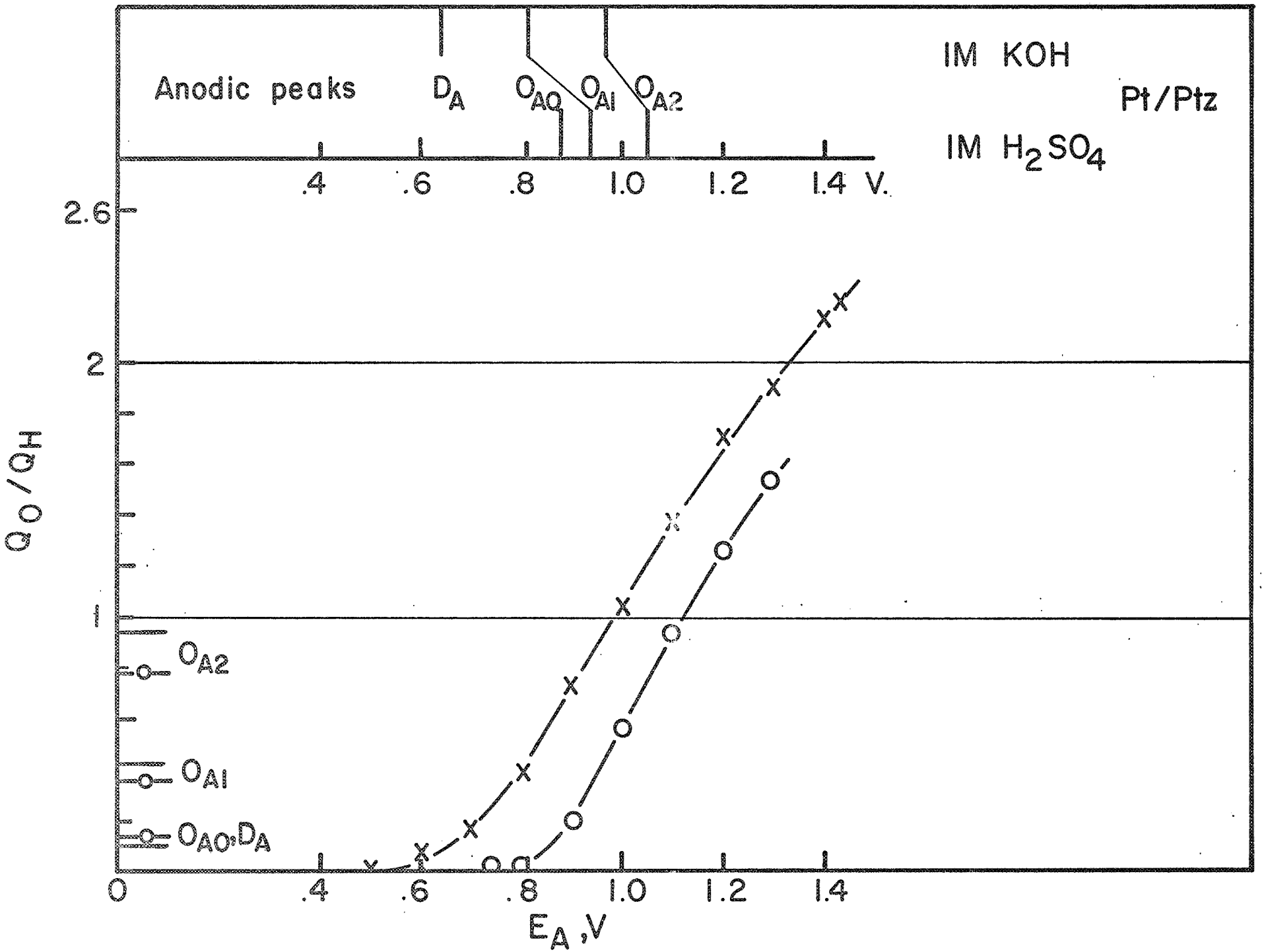
Anodic peaks
D_A
O_{A0}
O_{A1}
O_{A2}
IM KOH
Pt/Ptz
IM H_2SO_4
.4
.6
.8
1.0
1.2
1.4 V.
2.6
2
1
O_{A2}
O_{A1}
O_{A0}, D_A
Q_O/Q_H
0
.4
.6
.8
1.0
1.2
1.4
E_A, V

Figure 18

Relation between $\delta\Delta$, the change of ellipsometric parameter Δ, the phase shift, and the degree of surface oxidation of Pt and the corresponding potential. Note consistency of changes of Δ with degree of surface oxidation all the way down to $Q_O/Q_H = 0$ and inflection in the Δ relation at ca. 1.1 V.

Upper line is based on horizontal base-line for Δ as f(E); lower line is based on curved base-line for Δ as f(E); (the latter base line is the correct one on which changes of Δ are to be evaluated).

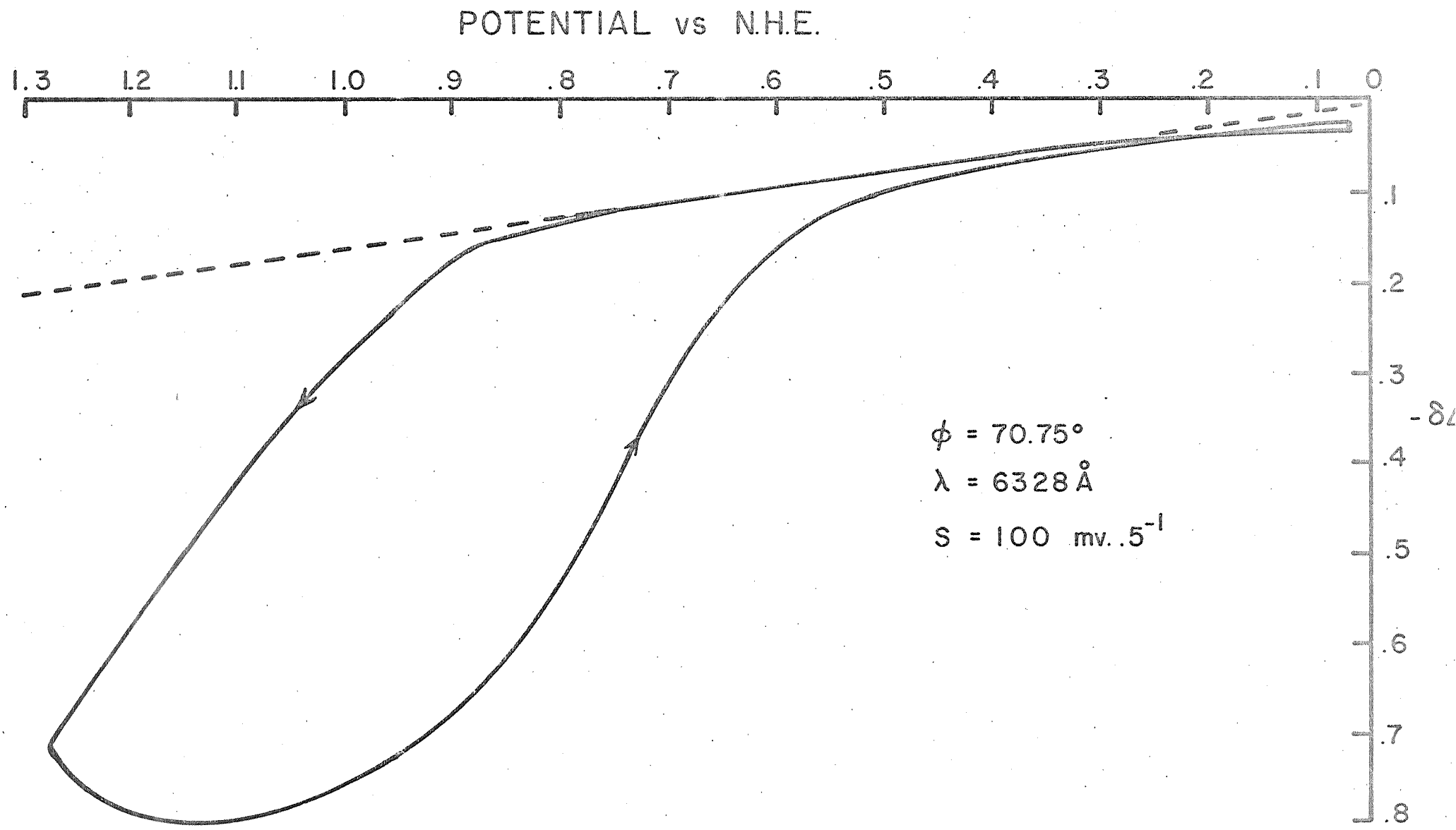
POTENTIAL vs N.H.E.
1.3
1.2
1.1
1.0
.9
.8
.7
.6
.5
.4
.3
.2
.1
0
.1
.2
.3
.4
.5
.6
.7
.8
- δ
ϕ = 70.75°
λ = 6328 Å
S = 100 mv. .5⁻¹

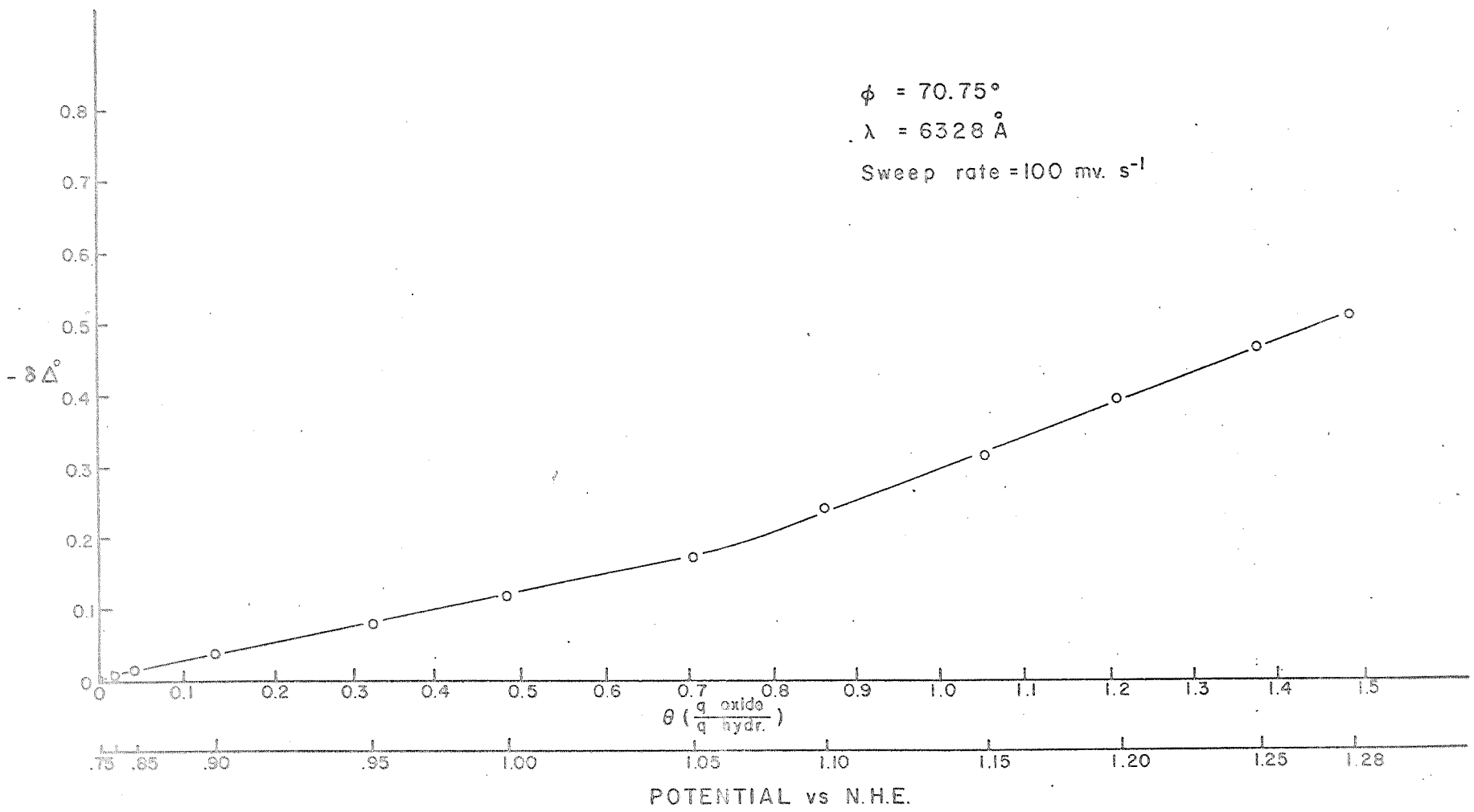
ϕ = 70.75°
λ = 6328 Å
Sweep rate = 100 mv. s^{-1}
$-\delta\Delta^{\circ}$
0.8
0.7
0.6
0.5
0.4
0.3
0.2
0.1
0
0
0.1
0.2
0.3
0.4
0.5
0.6
0.7
0.8
0.9
1.0
1.1
1.2
1.3
1.4
1.5
θ ($\frac{q \text{ oxide}}{q \text{ hydr.}}$)
.75
.85
.90
.95
1.00
1.05
1.10
1.15
1.20
1.25
1.28
POTENTIAL vs N.H.E.